CLASSIFICATION OF MARL PRAIRIE AND MARSH VEGETATION COMMUNITIES IN THE EVERGLADES NATIONAL PARK

By

ZOLTAN SZANTOI

A DISSERTATION PRESENTED TO THE GRADUATE SCHOOL
OF THE UNIVERSITY OF FLORIDA IN PARTIAL FULFILLMENT
OF THE REQUIREMENTS FOR THE DEGREE OF
DOCTOR OF PHILOSOPHY

UNIVERSITY OF FLORIDA

2011

To my family

ACKNOWLEDGMENTS

I would like to thank Dr. Scot Smith and the faculty of the School of Forest Conservation and Resources for the support and guidance during this endeavor. I also thank Dr. Francisco Escobedo, Dr. Amr Abd-Elrahman, Dr. Bon Dewitt, Dr. Franklin Percival and Dr. Leonard Pearlstine for serving on my committee and providing valuable assistance and encouragement throughout the entire process.

I would like to thank my parents and family for the support they have given for the past time, and most importantly to my wonderful wife, Joysee and son Zolta, for their love and support throughout the studies at the University of Florida. I would also like to thank my friends and colleagues for the great time we spent together.

TABLE OF CONTENTS

LIST OF TABLES

LIST OF FIGURES

LIST OF ABBREVIATIONS

ANN	Artificial Neural Network
ANOVA	Analysis of Variance
ASM	Angular Second Moment
AVHRR	Advanced Very High Resolution Radiometer
BP	Back Propagation
B&W	Black and White
CASI	Compact Airborne Spectrographic Imager
CART	Classification and Regression Trees
CHAID	Chi-squared Automatic Interaction Detector
CCD	Charge-Coupled Device
CERP	Comprehensive Everglades Restoration Plan
CIR	Color Infrared
CM	Tall Sawgrass Marsh
CWP	Short Sawgrass Prairie
DEM	Digital Elevation Model
DT	Decision Tree
EAA	Everglades Agricultural Area
EDEN	Everglades Depth Estimation Network
ENP	Everglades National Park
EVCS	Everglades Vegetation Classification System
ETM	Enhanced Thematic Mapper
GIS	Geographic Information System
GLCM	Grey Level Co-occurrence Matrix

GPS	Global Positioning System
HARN	High Accuracy Reference Network
ISODATA	Iterative Self-Organizing Data Analysis
J–M	Jeffries–Matsushita separability measure
ML	Maximum Likelihood
MLP	Multi-Layer Perceptron
MMU	Minimum Mapping Unit
MWP	Muhlenbergia Wet Prairie
NAVD88	North American Vertical Datum of 1988
NIR	Near Infrared
RMSE	Root Mean Square Error
QDA	Quadratic Discriminant Analysis
QUEST	Quick, Unbiased, Efficient Statistical Tree
SAR	Syntetic Aperture Radar
SCWP	Schizachyrium Wet Prairie
SB	Spectral Bands
SFWMD	South Florida Water Management District
VCS	Vegetation Classification System for South Florida National Parks
WP	Wet Prairie
Woody	Woody Vegetation

Abstract of Dissertation Presented to the Graduate School
of the University of Florida in Partial Fulfillment of the
Requirements for the Degree of Doctor of Philosophy

CLASSIFICATION OF MARL PRAIRIE AND MARSH VEGETATION COMMUNITIES IN THE EVERGLADES NATIONAL PARK

By

Zoltan Szantoi

August 2011

Chair: Scot Smith
Cochair: Francisco Escobedo
Major: Forest Resources and Conservation

This study developed a classification and discrimination methodology with quantifiable accuracies for wetland mapping, focusing on at risk plant communities in marl prairie and marsh areas of the Everglades National Park, Florida. Accurately and rapidly mapping the baseline spatial distribution of these communities with classification algorithms using accessible and temporally frequent imagery is critical to better assess changes in wet graminoid/sedge communities and their effects on the ecotone, wildlife habitats and overall ecological change. Maximum likelihood (ML), Decision Tree (DT) and Artificial Neural Network (ANN) classifiers were tested on high resolution aerial imagery (30.5 cm) of the Everglades National Park, Florida. Several parameters in the classification models were tested to improve mapping accuracy such as spectral bands, normalized difference vegetation index (NDVI) and first and second order texture features derived from the near-infrared band. The proper window size of the different texture features was estimated using the semivariogram method. The addition of NDVI and the texture features to the classification models yielded an increase in classification accuracy, especially in differentiating between wetland plant communities. Comparison

among the classifiers was based on the calculated Kappa coefficient of the developed maps. The results indicated that ANN classifier produced a statistically significantly higher accuracy (89.49%) than the DT (86.89%) or ML (84.92%) classifiers ($\alpha<0.05$). For delineating and mapping wetland plant communities, first and second order texture features derived from high resolution imagery improved the classification. Additionally, the utilization of machine learning algorithms (DT and ANN) in the classification process further increased overall accuracy of the developed maps. Findings from this study can be used to monitor vegetation communities in an accurate and efficient manner on a more frequent basis.

CHAPTER 1
INTRODUCTION

Wetlands are an essential part of the global ecosystem (Mitsch and Gosselink 2007) and provide habitat for endangered species, supply groundwater aquifers and have been reported to reduce floods (Nicholls et al. 1999; Winter 1999; Zedler 2000, 2003; Brinson and Malvárez 2002; Bullock and Acreman 2003; Hancock et al. 2005; Mitsch and Gosselink 2007). The Everglades is the only protected subtropical wetland ecosystem in the U.S and is located at the southern end of peninsular Florida covering about 10,100 km^2 from which 6108 km^2 is protected (Junk et al. 2006; Davis and Ogden 1994). The Everglades National Park is listed in the Ramsar Convention of Wetlands as being of International Importance (Richardson 2010) as well as in the UNESCO List of the World Heritage Sites in Danger (Ogden 2004). The area's distinct vegetation is a result of groundwater interactions and flow regimes (Harvey and McCormick 2009). The park has the largest mangrove forest in the western hemisphere and is the most significant breeding terrain for tropical wading birds as well as containing the largest continuous stand of sawgrass in North America (Ogden 2004). Because of its size location and climate, unique flora and fauna, hydrological functions and geological history, the Everglades has become one of the most studied ecosystems. According to Web of Knowledge ("Journal Citation Reports") the Everglades is the most extensively studied – and globally important – wetland. A literature search in April, 2011 identified 753 (66 in 2010) scientific papers for the Everglades in the wetland's topic, trailed by 234 (30 in 2010) in Brazil's Pantanal and 117 (11 in 2010) for the Okavango delta in Botswana.

America's largest subtropical wetland is in grave danger of degradation, due to numerous issues such as sea level rise, sedimentation, chemical pollution and human disturbance, climate change (Titus and Richman 2001; Ogden 2004; Pearlstine et al. 2010; Larsen et al. 2011) along with endangered species it provides habitat to the Florida panther (*Puma concolor coryi*), American crocodile (*Crocodylus acutus*) and Cape Sable seaside sparrow (*Ammodramus maritimus mirabilis*) (Walker and Solecki 2004). For example, ornithologists suggest that the region's wading bird population decreased by 90 to 95 percent since the pre-drainage era (Ogden 2004) and overall 68 native plant and animals found in the ENP are listed as endangered or threatened (Ogden 2004). The Biscayne aquifer which is located beneath the Everglades provides about 33% of the total public-supply groundwater in Florida and serves 4.48 million people (Marella 2009). Miami-Dade County itself withdraws all of its drinking water from the Biscayne aquifer which is more than 0.75 million cubic meters per day in 2005 (Marella 2009).

In recent years, in addition to water exploitation and land reclamation for urban development, the change to the hydrograph, and drainage canal construction combined with intense agriculture has led to increased disturbance, eutrophication and pollution of the Everglades ecosystem (Junk et al. 2006). Restoring the Everglades wetlands to their natural state is underway, not just to save the flora and fauna, but to ensure valuable water storage needed to maintain the quality of life in areas where population growth and development have substantially increased.

The major habitats and vegetation types in the Everglades are: sloughs, sawgrass marsh, wet prairies and tree islands (Richardson 2010). Sloughs have the longest

hydroperiods and deepest water levels with submerged vegetation and are found in the south-central and northeast Everglades. Sawgrass marsh is the main vegetation community in the park found throughout the area, dominated by Tall sawgrass (*Cladium jamaicense*) (Richardson 2010), however it is estimated that its extent is declining, making up only 38% of the 417,000 ha of historic sawgrass-dominated areas (Davis et al. 1994). Sawgrass, which is sedge, can occur in pure dense or sparse complexes or is mixed with other sedges, grasses, small shrubs, and attached emergent or floating plants (Richardson 2010). The nearly total dominance of sawgrass is one of the distinguishing features of the Everglades (Kushlan 1990).

Wet prairies comprise the second most abundant vegetation community, and are found mainly in the northern and central portion of the park (Gunderson and Loftus 1993). These communities typically consist of relatively low growing emergent plant species such as *Rhynchospora*, *Panicum* and *Eleocharis*. The water depth in the wet prairies is generally deeper than sawgrass marshes but shallower than sloughs. However, while sawgrass marshes are inundated 6-9 months per year, wet prairies are usually flooded less than 6 months (Kushlan 1990).

Tree islands are scattered throughout the park, dominated by a mixture of trees, shrubs and ferns. Tree islands are the highest elevation land features in the Everglades, even though they are elevated only slightly above the surrounding wetland (Willard et al. 2006) with elevations ranging from 0.2 m to 1.5 m above the sloughs and cover less than 5% of the park (Sklar and van der Valk 2002).

Wet graminoid communities in the wet prairie and sawgrass marsh mosaic cover the largest portion of the Everglades ecosystem and shelter 44% of the remaining

618,000 hectares of the Everglades National Park (Davis et al. 1994). Wet graminoid communities provide habitat, shelter and food for their numerous inhabitants including white-tailed deer (*Odocoileus virginianus*), Florida panther (*Puma concolor coryi*), bobcat (*Lynx rufus*), and raccoon (*Procyon lotor*) Cape Sable seaside sparrow (*Ammodramus maritimus mirabilis*), Wood Stork (*Mycteria americana*), cottonmouth snake (*Agkistrodon piscivorus*) soft-shelled turtle (*Apalone ferox*) crayfish (*Procambarus alleni*) (USFWS 1999).

The continuous degradation of the wet graminoid communities adjacent to the urban-rural interface and inner sections in the national park (Davis et al. 1994; Richardson 2010), warrants rapid and repeatable monitoring to better understand changes in their size and flora. These communities will be the first to change in response to restoration, hydrological changes, climate change or other impacts such as fire, hurricanes and nutrient input (Gunderson 1997; Armentano et al. 2006; Zweig and Kitchens 2008). So, it is important to rapidly and regularly assess flora and fauna changes to prevent further degradation. Armentano et al. (2006) predicted that observable change like shifts in species dominance in wet prairie and marsh vegetation may occur in a few years due to changes in hydrological regimes, where the once dominant muhly grass (*Muhlenbergia capillaries*) was replaced by sawgrass (*Cladium jamaicense*).

Besides hydrological changes, nutrient availability and fire are considered the most important influences on wetland vegetation in the Everglades (Doren et al. 1997; Childers et al. 2003; Lockwood et al. 2003). Historically the Everglades was a phosphorus limited ecosystem (Richardson and Huvane 2008; Richardson 2010).

However, nutrient loading from the Everglades Agricultural Area (EAA) and adjacent urban areas have significantly increased nutrient concentrations, particularly phosphorous (Davis 1994a; Stober et al. 1996; Richardson 2010). The nutrient loading resulted in increased water phosphorous content, changed periphyton communities, and has led to loss of native saw grass communities, increased organic matter in water, loss of dissolved oxygen, conversion of wet prairie plant communities to cattails, and loss of important wading bird habitats (Stober et al. 1996; Richardson 2010).

Olmsted and Armentano (1997) emphasized that accurate spatial data on vegetation distribution is key to understanding and detecting changes in ecosystem structure and extent at the local and landscape scale in the Everglades. Frequent high-density in-situ monitoring of the park would be prohibitively costly and time-consuming. But, an accurate map developed from aerial or satellite imagery could be used to more rapidly detect and monitor spatial and temporal changes in the wetland graminoid communities' and assess degradation. However, identifying and distinguishing wet graminoid communities in the Everglades using aerial or satellite imagery is difficult because of the color similarity between these communities (Olmsted and Armentano 1997).

Several vegetation classification systems (Florida Fish and Wildlife Conservation Commission, Florida Land Use and Cover Classification System, Florida Gap Analysis Project and Vegetation Classification System for South Florida National Parks) (Duever 2006) have been developed and used to map the ENP. One of the most detailed vegetation map for the ENP was produced in 1994 (Madden et al. 1999), using the Vegetation Classification System for South Florida National Parks. The study was

conducted in the late 1990's and used direct photo-interpretation of 1:40,000-scale color infrared (CIR) film-based vertical aerial photographs (Madden et al. 1999). In 2004 a new set of color infrared imagery was taken at the 1:24,000 scale. The imagery from the 2004 mission is currently being processed employing visual photo-interpretation method to produce a new vegetation map for the Park. The latest aerial imagery which covers the entire ENP was done in April 2009. The South Florida Water Management District (SFWMD) requested the imagery in the framework of the Comprehensive Everglades Restoration Plan (CERP) program which requires a periodical vegetation map for the Everglades to assess the system-wide performance of the CERP (http://www.evergladesplan.org/index.aspx).

Since the latest comprehensive mapping effort (Madden et al. 1999) was conducted, a number of technological advancements have been made in remote sensing technology. Digital cameras are replacing film-based cameras, computer based image classification techniques are used instead of human photo-interpretation, images can now be radiometrically enhanced and the spatial accuracy in the imagery has greatly increased. This project will apply these new technologies and techniques in a pilot study to (1) test the use of high resolution aerial imagery, (2) assess the usefulness of texture features derived from spectral data, (3) analyze classification algorithms and (4) determine acquisition times for large scale implementation of these techniques. The results of this study will assess which data sets or algorithms are better suited for the large scale mapping implementation in the ENP.

Objectives

1. To determine whether graminoid/sedge (Sawgrass marsh, Sawgrass wet prairie, Schizachyrium wet prairie, Muhlenbergia wet prairie) communities can be discriminated based on spectral and textural properties.

2. Assess the accuracy of using Back Propagation Artificial Neural Network and QUEST Decision Tree classification algorithms in classifying graminoid/sedge plant communities.

Significance of the Study

This study developed a repeatable classification and discrimination methodology with quantifiable accuracy for wetland mapping and monitoring of at risk plant communities in marl prairie and marsh areas. Based on the findings, a classification plan/scheme was developed by which these vegetation communities could be monitored in an accurate and efficient manner on a regular basis, and an accurate, current map of the graminoid communities produced for the study area in the Everglades.

The recently proposed expansion of the ENP by the State of Florida will significantly increase the area of the park (Stokstad 2008). This study's results provide detailed information on vegetation patterns, including wetland communities which are the major factor in evaluating alteration in wildlife habitats and ecological change. This research is essential to better understand spatial and temporal changes in vegetation cover, monitoring of hydrologic restoration of the acquired areas, and detect change on the existing area (Olmsted and Armentano 1997). An annually updateable vegetation database for the ENP will offer an optimal solution to track and monitor changes in the ENP's vegetation communities.

For example, Doren et al. (1999) calculated that the cost to develop such a database for the less fragmented and more homogenous Water Conservation Area 1, which is located approximately 70 km northeast of the ENP is about $7.20/ha ($9.66 in 2011, based on the U.S. Bureau of Labor Statistics's Consumer Price Index Data). Employing a commercial firm with this unit cost would roughly translate to a cost of

$14,000,000 ($18,800,000 in 2011 dollar terms) to map the entire ENP. In a recent study Rutchey and Godin (2009) estimated a cost of over $59,000,000 to map the ENP with a 10 m x10 m minimum mapping unit (MMU) using photo interpretation techniques. Because of cost and precision factors, Rutchey and Godin (2009) recommended developing a vegetation map with 50 m x 50 m MMU, which would costs about $560.00 per hectare. However, the authors also mentioned that field ecologists usually require finer MMU (i.e. 2m x 2m). Therefore to provide more accurate maps and change detection products for local scale studies, investigating plant community shifts, and when capturing spatial heterogeneity is very important, a map using the original pixel size as the minimum MMU is a suitable option to reduce the loss of specificity introduced in the resampling process (Knight and Lunetta 2003).

CHAPTER 2
LITERATURE REVIEW

Remote Sensing of Wetlands

Remote sensing techniques have been used to provide rapid and comprehensive representation of plant communities in marsh and wet prairie (Reed 1988; Sader et al. 1995; Smith et al. 1998; Harvey and Hill 2001; Belluco et al. 2006; Johansen et al. 2007; Dillabaugh and King 2008; Maxa and Bolstad 2009). However, the spectral similarity between marsh and wet prairie communities has prevented high classification accuracy (typically above 80%) using single remote sensing data sources (spectral bands) or standard classification approaches such as Iterative Self-Organizing Data Analysis (ISODATA) (Reed 1988; Sader et al. 1995). Additionally, significant shifts towards drier vegetation communities such as Muhlenbergia wet prairie, Schizachyrium wet prairie and tree islands in the Everglades has occurred since the last mapping effort due to urbanization, anthropogenic drainage activities, climate change (Duever 2005; Ogden 2005; Willard et al. 2006; Richardson and Huvane 2008; Bernhardt and Willard 2009; Pearlstine et al. 2010). These rapid ecological changes illustrate the need for more accurate and automated classifications methods.

Previous studies have been done to map wetland plant communities using different remote sensing platforms and techniques (Madden et al. 1999; Belluco et al. 2006; Gilmore et al. 2008). Ozesmi and Bauer (2002) reviewed the literature on remote sensing of wetlands and found that one of the main problems is the spectral separability of specific wetland vegetation classes. Schmidt and Skidmore (2003) reported that mapping major physiognomic or forest type classes is fairly straightforward and provides good, accurate results, while differentiating between grasses or sedges was

difficult because of the very similar reflectance wavelengths of these communities. Gluck et al. (1996) found that, indeed, spectral separability of different wetland types is a problem due to the overlap among their spectral signatures. As a limitation of satellite remote sensing, Ozesmi and Bauer (2002) concluded that at medium spatial resolution, it is difficult to identify wetland types. Moreover, because most satellites are on a fixed orbit and return intervals, it is difficult to capture optimal lighting and water level conditions for wetlands. They suggested aerial photography as the preferred image type for detailed wetland mapping. Dahl (2006) agreed that high resolution satellite imagery can be an effective remote sensing platform for wetland mapping.

Textural Features

Spectral features describe the average tonal variations in various bands of the visible and infrared portion of an electromagnetic spectrum, whereas textural features contain information about the spatial distribution of tonal variations within a band (Haralick et al. 1973). When a pixel is viewed in context with its surrounding pixels, a pattern may emerge that is consistent with a cover type yet different from other cover types. High resolution imagery could provide significant feature variables based on first and second order texture analyses (Wang et al. 2004). This sort of contextual identification can improve the accuracy of image classification and is essential for classification of high resolution images (Ge et al. 2006; Waser et al. 2008).

Texture is a statistical property of the spatial distribution of image spectral tones (Haralick et al. 1973). First order statistics quantify the distribution of spectral tone properties in the image for a given neighborhood while second order statistics describe the frequency with which one gray tone appears in a specific relationship to another gray-tone in the image and they are calculated from the grey-level co-occurrence matrix

(GLCM). The GLCM indicates the probability of each pair of pixel values (*i*, *j*) co-occurs in a given direction and distance (Haralick et al. 1973). These measures can be calculated in four directions (horizontal, vertical, left diagonal, right diagonal) on the image and are then averaged (Haralick et al. 1973). The most common and successfully used first order statistics in classification studies are the mean and standard deviation (Pearlstine et al. 2005; St-Louis et al. 2006; Berberoglu et al. 2007; Ashish et al. 2009).

The fourteen second order statistics that Haralick et al. (1973) defined are often statistically correlated. Overall, several studies (Baraldi and Parmiggiani 1995; Wulder et al. 1998; Clausi 2002; Puissant et al. 2005) attempted to find the most appropriate second order texture features for image classification. Baraldi and Parmiggiani (1995) found that angular second moment (ASM), contrast and correlation were the least correlated among the fourteen second order texture features. Wulder et al. (1998) tested Haralick's texture features and found that homogeneity, contrast, dissimilarity, and entropy were useful. Although Clausi (2002) recommended contrast, correlation and entropy; Puissant et al. (2005) recommended homogeneity. For vegetation mapping applications both first order statistics such as the mean and standard deviation and second order statistics have been employed (Pearlstine et al. 2005; Dillabaugh and King 2008; Ashish et al. 2009). Based on previous research findings (Baraldi and Parmiggiani 1995; Wulder et al. 1998; Pearlstine et al. 2005; Puissant et al. 2005; Ashish et al. 2009), mean, standard deviation, ASM, dissimilarity, homogeneity and entropy are calculated and tested for each of the digital image (red, green, blue and infrared) bands.

Photo Interpretation

Visual photo interpretation has been used in several studies (Madden et al. 1999; Rutchey et al. 2008; Maxa and Bolstad 2009) with good overall accuracy results. Ground collected datasets were used in these studies to evaluate the accuracy of the developed maps. However, photo interpretation is extremely time and labor consuming, and highly dependent on the photo interpreter skills and knowledge of the area (Ozesmi and Bauer 2002). Most image classification costs incurred in using digital aerial photography for land cover mapping is not in obtaining the imagery, but in the interpretation process, especially when more than one photo interpreter is involved (Joria 2001).

As resources become scarce and the need for rapid land cover assessment becomes more necessary, government and non-government agencies are ever more interested in finding more effective and less costly methods of obtaining land cover information (Joria 2001). Automated interpretation of digital aerial photographs has a strong potential for offering an alternative to the visual photo interpretation process because of its reliability, repeatability and processing speed (Joria 2001). Puig et al. (2002) also noted that visual photo interpretation is the preferred method for analyzing land cover in low and medium resolution satellite imagery in a tropical setting, but its application is limited to high spatial resolution imagery because of the increased need for detail to facilitate recognition. Baker et al. (2006) also found that comparison of multispectral image classification of wetlands has similar accuracy and greater repeatability to human interpretation. Automated remote sensing techniques such as Maximum likelihood (ML), Decision trees (DT) and Artificial Neural Networks (ANN)

(Wang et al. 2004; Baker et al. 2006; Belluco et al. 2006; Wright and Gallant 2007; Sesnie et al. 2008) are reliable alternatives in wetland inventory and mapping.

Automated Image Classification Techniques

As mentioned above, a great number of remote sensing techniques have been used to differentiate land cover types using space or airborne imaging sensor data in combination with several classification procedures. Maximum likelihood is regarded as a common and widely used supervised classification algorithm for satellite and airborne image classification (Lu and Weng 2007). It is based on normal distribution assumption where the algorithm uses the mean and variance of the collected training data to estimate the probability that a particular pixel belongs to a category or class.

New methods, such as decision trees and neural networks, have been introduced in the last decade (Tso and Mather 2009). Decision trees and ANNs become especially popular because they are non-parametric models, thus make no assumption about the statistical distribution of the data (Richards and Jia 2006). Ozesmi and Bauer (2002) also noted that when using automated techniques such as ML, DT, ANN methods, ancillary data such as image texture information (Haralick et al. 1973), can be incorporated into the analysis in addition to multispectral data, and in most cases, can improve classification outcomes (Ghedira et al. 2000; Wang et al. 2004; Fuller 2005; Wright and Gallant 2007; Dillabaugh and King 2008; Sesnie et al. 2008). Wang et al. (2004) for example, incorporated first and second order texture features into his ML classification model and his results indicated that texture increased the classifier accuracy. Sesnie et al. (2008) achieved 12% higher overall accuracy when DEM and climate related ancillary variables were used in addition to multispectral bands in a classification tree analysis. Dillabaugh and King (2008) incorporated Normalized

Difference Vegetation Index (NDVI) into their model and found it useful in improving classification accuracy relative to using solely spectral band combinations. Wright and Gallant (2007) tried to discriminate five palustrine wetland types. When image texture features, DEM and ancillary GIS data (DEM, habitat and cover type) were added to the multispectral data, the average overall error rate dropped incrementally. However, Michishita et al. (2008) compared decision tree classifier with ancillary (e.g. DEM and land surface temperature and other spectral indices) data against the ML classifier at the wetland plant family level and found that ML performed slightly better. Michishita et al. (2008) argue that the lower accuracy was due to the low number of training pixels used for most of the studied vegetation classes. In general, we can surmise that first and second order image texture features can increase image-based wetlands classification.

Artificial Neural Networks has become an important part of remote sensing image classification because they can handle complex and very large datasets efficiently and in many cases, produce more accurate results than traditional classifiers (e.g. ML or non-parametric parallelepiped classifiers (Moody et al. 1996). Artificial Neural Networks technology has drawn significant interest in recent years and are being used in landcover mapping (Paola and Schowengerdt 1995; Berberoglu et al. 2007; Ashish et al. 2009) frequently, but literature on their application and use in wetland mapping is limited (Ghedira et al. 2000; Mas 2004; Fuller 2005; Dillabaugh and King 2008). So, these studies indicate that ANN can be used to improve vegetation discrimination with various success rates.

In a recent land-use classification study Ashish et al. (2009) employed probabilistic ANN using 1 meter resolution multispectral image and second order texture features (Haralick et al. 1973) in the classification process. The overall accuracy when image texture was involved was 89%. Berberoglu et al. (2007) tested several texture features for landcover mapping with ML and ANN classifiers. Artificial Neural Networks outperformed the ML classifier in the overall classification accuracy without texture data using Landsat spectral bands. The authors also reported that ANN performed better when texture data was incorporated into the classification; however the overall accuracy slightly decreased for agricultural (citrus plantation, first crop corn, second crop corn, cotton, soil, soya, water and urban) and semi-natural (bulrush, cotton, dune vegetation, salty plain, dune, soil, wet soil, wetland and water) landcovers. Ghedira et al. (2000) attempted to distinguish between wetland categories using the ANN back propagation algorithm on texture information of RadarSat SAR (Canadian Space Agency) data. When texture was included in the analysis, 99.8 percent of the pixels were classified, and less than 3 percent of the total number of pixels were classified as a mixed class (shrubby and woody wetland). Mas (2004) used Landsat imagery to map land cover classes in a tropical, coastal area by employing ANN and ancillary data such as elevation and soil data. Model output was compared with output from spectral classification and a significant increase in accuracy of the land use classification (from 67% to 79%) was detected. Multispectral IKONOS imagery was used by Fuller's (2005) to detect invasive Melaleuca trees (*Melaleuca quinquenervia*), sawgrass and 3 other classes in South Florida. Back propagation ANN was employed as well as spectral bands, texture layer and normalized difference vegetation index as input layers. The

author achieved over 85% overall accuracy, however a visual inspection revealed that a class called “other woody type” was frequently misclassified as Melaleuca class. However, Dillabaugh and King (2008) attempted to map wetland composition using Back Propagation ANN based on high resolution satellite imagery (IKONOS) and concluded that ML classifier performed better than the artificial neural network classifier.

Most of these studies above utilized satellite or hyperspectral imagery with variant spatial resolution. The delineation of wetlands as single landcover was frequently the objective of these studies, rather than delineation of vegetation classes or species within wetlands. Therefore, the purpose of this study is to determine the applicability of multiple classification algorithms such as decision trees and neural networks to delineate the ENP’s dominant graminoid communities using high resolution aerial imagery and texture features.

Hypotheses

1. Classification accuracy of grass/sedge communities will be statistically significant using texture features at an alpha of 0.05 level.
2. Machine learning image classification methods can discriminate graminoid communities more accurately than the traditional Maximum Likelihood statistical classifier algorithm at an alpha of 0.05 level.

The classification accuracy of the developed maps was assessed using confusion matrices, where user’s, producer’s and overall accuracy values were calculated and presented. Kappa coefficients (Foody 2004) to evaluate the difference between two thematic maps were also calculated. To compare the kappa coefficients, z-tests were performed to test the hypothesis whether the results of two classifiers differ significantly (Donner et al. 2000).

Study Area

The study site is located in the eastern portion of the ENP as shown in Figure 2-1 (Miami-Dade County). The area was selected because of its diversity of land cover types including spatially mixed marsh and marl prairie but homogeneous communities as well. The area was also selected because recent baseline data (Ross et al. 2003; Ross, Sah, et al. 2006; Ross, Mitchell-Bruker, et al. 2006) of these vegetation communities exists. The terrain of the study area is flat. Elevation varies between 0 and 0.6 meter.

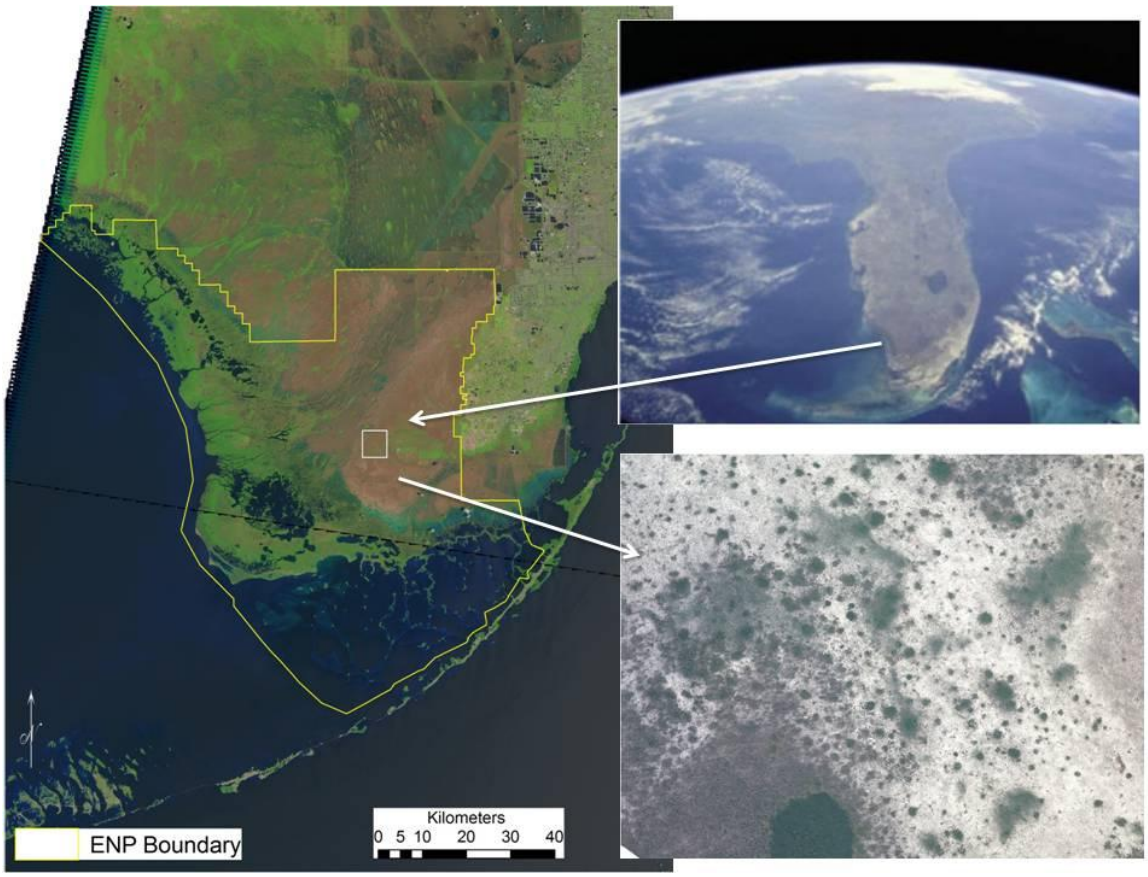

Figure 2-1. Study area within the Everglades National Park, Florida USA

CHAPTER 3
WETLAND COMPOSITION ANALYSIS USING HIGH RESOLUTION IMAGES AND TEXTURE FEATURES

Introduction

Wetlands cover 6% of the world's surface, contain about 12% of the global carbon pool and play an important role in the global nutrient and carbon cycles (Erwin 2008). One of the biggest concerns in regard to climate change effects is the status of wetlands regarding nutrient (nitrate, iron, and sulfate) dynamics and matter fluxes (Paul et al. 2006; Erwin 2008). The Everglades are being subjected to numerous detrimental effects such as sea level rise, sedimentation, chemical pollution, human disturbance, and climate change effects (Titus and Richman 2001; Ogden 2004; Pearlstine et al. 2010; Larsen et al. 2011). These are affecting endangered species' habitats such as those of the Florida panther (*Puma concolor coryi)*, American crocodile (*Crocodylus acutus*) and Cape Sable seaside sparrow (*Ammodramus maritimus mirabilis)* (Walker and Solecki 2004). In addition, the past decade, the growth of the Miami-Fort Lauderdale metropolitan area in the last decade, intense agriculture activities in the Lake Okeechobee area and human-induced changes in the hydrological system have caused significant disturbance in the Everglades ecological system (Junk et al. 2006; Marella 2009; Richardson 2010). Restoring the Everglades wetlands to their natural state is in progress to not only to save the flora and fauna, but to ensure valuable water storage and improve living conditions in areas with changing population growth and development (Richardson 2010).

Wet graminoid communities (e.g. marl prairies and marshes) cover the largest portion of the Everglades ecosystem (Davis et al. 1994) and provide living area, shelter and food for their animals. These communities suffer continuous degradation from being

close to the urban-rural interface, as well as in some developed inner sections of the Everglades National Park (ENP). Changes in graminoid community distribution could be used to provide advanced warning or indicators of ecological disturbance and more severe ecological shifts due to climate and/or land use changes (Goodin and Henebry 1997; Pearlstine et al. 2010). Monitoring these graminoid communities could also serve as advanced warning against expected sea level rise and a tool to better assess and evaluate restoration efforts. Olmsted and Armentano (1997) stressed the disturbance monitoring concept and confirmed that accurate spatial data on vegetation distributions is key to understanding and detecting changes in ecosystem function at the local and landscape levels. In fact, the discrimination of wet graminoid communities using remote sensing technologies has been the most frequently cited challenge in past attempts at land cover classification in many areas worldwide including the Everglades (Ozesmi and Bauer 2002).

Remote sensing techniques have been used to provide rapid and comprehensive discrimination of plant communities, including marsh and wet prairie (Smith et al. 1998; Belluco et al. 2006). However, the spectral similarity and inter-digitations between these two communities prevented high classification accuracies using a single remote sensing data source (spectral bands only) or standard classification approaches such as unsupervised or parallelepiped classification. Although vegetation maps for the ENP have been reported to have low classification accuracies, there is an ongoing shift toward drier vegetation communities (Armentano et al. 2006). Accuracy assessment results of data collected through direct visual interpretation of 1:40,000 scale vertical, Color Infrared (CIR) aerial photographs taken in the mid-1990’s (Welch et al. 1995) in

the ENP found a 25% error in the classification of Tall sawgrass communities, 33% error for Short sawgrass and 60% error for muhly grass/marl prairie.

Spatial resolution is one of the most significant factors that influences image classification accuracy. Yang (2007) demonstrated the significance of high spatial resolution (2m) scanned, ortho-rectified color aerial images in accurately classifying riparian zone vegetation when compared to Satellite for the Observation of the Earth (SPOT) - 4 and Landsat-7 Enhanced Thematic Mapper (ETM+) imagery. The overall accuracy of the high resolution aerial imagery results was 81% while Spot-4 and Landsat-7 provided 63% and 53% overall accuracy. Maheu-Giroux and Blois (2005) used scanned black and white (B&W) and color aerial photos (0.33m ground resolution) to discriminate common reed (*Phragmites australis*), an invasive plant, from other types of vegetation. They achieved an overall accuracy between 71%-87% for panchromatic image analysis and 77%-88% for color imagery. However, when both results were compared, it was evident that the differences were not statistically significant. Dillabaugh and King (2008) used the spectral bands of IKONOS imagery (4 meter resolution) to discriminate wetland vegetation types. The overall accuracy of their classification increased when the Normalized Difference Vegetation Index (NDVI) was included in the analysis.

High-resolution imagery provides better discrimination of significant features beyond their spectral content represented by their first and second order texture features (Haralick et al. 1973; Wang et al. 2004). This sort of contextual identification can improve the accuracy of image classification of high-resolution images (Ge et al. 2006; Waser et al. 2008). Moreover, in digital image processing and remote sensing

data analyses, the spatial neighborhood of a pixel may provide even more information than the pixel itself (Dell'Acqua et al. 2006). Spectral features describe the average tonal variations in various bands of the visible and infrared portions of the electromagnetic spectrum, whereas textural features contain information on the spatial distribution of tonal variations within a band (Haralick et al. 1973). When a pixel is viewed in context with its surrounding pixels, a pattern may emerge that is consistent with a landcover type and different from other types, thereby facilitating discrimination (Pearlstine et al. 2005).

The most commonly used first order textural statistics used for most classification studies are the range, mean, standard deviation/variance, skew and entropy (Coburn and Roberts 2004; Pearlstine et al. 2005; St-Louis et al. 2006; Ashish et al. 2009). In Coburn and Roberts' (2004) study, the authors found that inclusion of variance significantly increased the classification accuracy of landcover classes by 9%. Pearlstine et al. (2005) concluded that the mean and standard deviation were very effective in discriminating Brazilian pepper (*Schinus terebinthifolius*) from other type of vegetation. St-Louis et al. (2006) used first order texture measures to predict bird species richness and reported that range and standard deviation were significant predictors. Ashish et al. (2009) also observed that mean and standard deviation increases the overall mapping accuracy.

Baraldi and Parmiggiani (1995) found that angular second moment (ASM), contrast and correlation provided the best results when testing it on an Advanced Very High Resolution Radiometer (AVHRR) using cluster analysis. Wulder et al. (1998) tested Haralick's texture features using compact airborne spectrographic imager (CASI)

imagery, and found that homogeneity, contrast, dissimilarity, and entropy were useful. Clausi (2002) recommended contrast, correlation and entropy based on Synthetic Aperture Radar (SAR) imagery and maximum likelihood classifier, while Puissant et al. (2005) recommended the use of homogeneity texture feature using SPOT-5 imagery. Since textural features are scale dependent, determining the optimal window size to extract these features is important (Puissant et al. 2005; Tso and Mather 2009). In general, a larger window size performs better and is needed for higher resolution imagery and for spatially heterogeneous classes. On the other hand, a small window size yielded higher accuracy for spatially homogeneous classes (Ashish et al. 2009). However, if the window size is too small relative to the examined texture feature, the real property of the texture feature will not be accurately reflected (Tso and Mather 2009). A 3x3 window size is generally preferred for first order texture feature extraction (Berberoglu et al. 2007). Different window sizes have been used to extract second order texture statistics (Wang et al. 2004; Puissant et al. 2005; Ge et al. 2006; Ashish et al. 2009).

Finding the most appropriate window size for the appropriate scale (Dell'Acqua et al. 2006) for better achieving the highest classification accuracy is difficult. Semivariograms have been extensively used in remote sensing studies to calculate optimal neighborhood size (Franklin et al. 1996; Dell'Acqua et al. 2006; Johansen et al. 2007; Balaguer et al. 2010). Franklin et al. (1996) successfully used semivariogram range to estimate the optimal window size by calculating the semivariance for different vegetation classes in an image. They concluded that the semivariogram range can be a useful guide for selecting the appropriate texture window size. Semivariance is typically

expressed as a semivariogram curve that depicts its values at different lag distances. In a typical semivariogram, the semivariance values increase with the increase of the lag distances up to a certain distance (range) where the values are no longer correlated with the lag distance and thus provide a measure of the size or scale of the largest and most dominant elements in the scene (Curran 1988). Franklin et al. (1996) also concluded that the semivariogram range can be useful as a guideline for selecting the appropriate second order texture window size.

This study's aim was to develop a method for utilizing spectral and textural characteristics of high resolution digital aerial imagery to better discriminate between marl prairie and marsh plant communities in the ENP. These plant communities have been reported as difficult to classify due to their spectral similarity (Olmsted and Armentano 1997). Thus, the main hypothesis of this research is to determine if first and second order textural features lead to significant improvement in the classification accuracy. Specifically, this study used multiple combinations of spectral and textural features as additional dimensions to improve classification accuracy. Multiple window sizes for first and second order texture features were also tested to identify optimal parameters for achieving the highest classification accuracy.

Methods

Classification Scheme

Several vegetation classification schemes (Florida Gap Analysis Project, Florida Land Use and Cover Classification System, Florida Fish and Wildlife Conservation Commission, Multi-Species Recovery Project, and Vegetation Classification System for South Florida National Parks) (Duever 2006) have been used to classify the ENP plant communities. This study employed a modified version of the Vegetation Classification

System for South Florida National Parks (VCS) (Rutchey et al. 2006). This system was developed by the South Florida Natural Resources Center, the Center for Remote Sensing and Mapping Science at the University of Georgia, Big Cypress National Preserve and the South Florida Water Management District (Rutchey et al. 2006). The major vegetation types in this system are hierarchically arranged plant communities which are defined by the dominant vegetation species. However, the “prairies and marshes” major vegetation type needs additional classes to better separate graminoid wet prairie and marsh communities as shown in Table 3-1. Most marsh types were dominated by fewer than 10 species (Kushlan 1990; Craft et al. 1995; Olmsted and Armentano 1997) while wet prairies have much higher species richness (Olmsted et al. 1980). Table 3-1 also contains the major plant species in the study site (Ross et al. 2003; Ross, Sah, et al. 2006).

Study Area and Field Data Collection

The 8.5 km² study area was flat and had elevation ranging from 0 to 0.6m above sea level and is located in the south eastern portion of the ENP (25º25´09.09´´ to 25º24´15.16´´ N and 80º46´41.46´´ to 80º45´41.00´´ W) as shown in Figure 3-1. The study area was selected because of its existing land cover, which includes an intermix of distinct marsh and marl prairie communities. The study area has been previously studied as part of baseline studies of the Everglades’ ecological systems and other restoration efforts (Ross et al. 2003). This study utilized a dataset collected in the spring of 2008 by scientists from Florida International University (Dr. Mike Ross and Michael Kline, personal communication) as well as data from existing plots that were revisited and measured in the spring of 2009. These data sets were collected using Trimble Pathfinder GPS units (accuracy < 0.5m) and included information about the plant

communities (Table 3-1), water levels, and soil depths. Additional ground reference information for the studies' plant communities was collected using real time kinematic GPS unit (TOPCON Hiperlite, minimum accuracy of < 0.1m) at the time of image acquisition.

In general (Tso and Mather 2009) suggest that for a statistical classifier, at least 30 times the number of feature classes (i.e. number of bands) is needed to determine the number of training data pixels per class. The training dataset collected as GPS points were extrapolated into polygons using visual image interpretation to include a sufficient number of pixels in the analysis (Table 3-2). Based on the proposed five-class classification scheme (see Table 3-1), the number of feature classes (15 spectral and texture features) and Tso and Mather (2009) suggestion regarding training data size, a minimum of 450 pixels were selected (Table 3-2) as a training set for each class. Each training and accuracy polygon contained a minimum of 297 pixels. The training areas for each class were larger than the minimally determined pixel number (450) to acquire statistically significant number of pixels for each class as well as to get good representation of the class spectral reflectance values. Two-thirds of the ground truthing data were used to train the classifier while the remaining third was set aside to test classification accuracy.

Imagery

The images used in this study were collected using Microsoft Vexcel's UltracamX camera in the spring of 2009. The main characteristics of the imagery are summarized in Table 3-3. Natural color and color infrared imagery were collected over the ENP. For the UltracamX camera, a separate sensor was used to collect each spectral band, with the optical path passing through a filter, lens assembly, and a Charge-Coupled Device

(CCD) array. These bands are collected when the image gets triggered during the survey flight. All images were free of smoke, clouds and cloud shadows. The images were acquired while the solar elevation angle was greater than 30° above the horizon. They were collected in the spring during spring – leaf on – conditions. The images were geometrically and radiometrically corrected and pan sharpened (UltracamX system data level-3). No orthorectification was performed; however, geometric distortions due to relief change were ignored because of the minimal elevation relief found in the study research area (Wolf and Dewitt 2000).

Geo-referencing of the imagery was accomplished via direct referencing using post processed airborne global positioning systems (GPS) and inertial measurement unit data supplier, Aerial Cartographics of America, Inc. Orlando FL. The horizontal positioning accuracy of the imagery was 3.00m with a 95% confidence interval (Root Mean Square Error, RMSE = 1.76m given that positional accuracy = 1.7308 * RMSE). Imagery was in the State Plane Coordinate System, Florida East Zone 0901, North American Datum of 1983/High Accuracy Reference Network (HARN). Imagery was mosaiced to construct a single image covering the entire study area and clipped to save file space and to eliminate the portion of the images beyond the area of interest (Figure 3-2).

Development of Texture Features

First-order statistics (i.e. data range, mean, variance and entropy) were used to quantify the distribution properties of the image spectral tone for a given neighborhood (Haralick et al. 1973). Second-order statistics (i.e. mean, variance, homogeneity, dissimilarity, entropy and angular second moment) described the frequency with which one gray tone appears in specific relationship to another gray-tone in the image. These

features were calculated from the grey-level co-occurrence matrix (GLCM) extracted from an image neighborhood (moving window). The GLCM indicates the probability that each pair of pixel values co-occurs in a given direction and for certain lag distance in the image (Haralick et al. 1973).

Texture measures were calculated in four directions (horizontal, vertical, left diagonal, right diagonal) and averaged (ITT ENVI software). Out of the fourteen second–order statistic texture features that Haralick et al. (1973) defined, many were correlated. Thus, the mean, variance, homogeneity, dissimilarity, entropy and ASM were calculated and tested for the near infrared bands. The spectral bands of the imagery were highly correlated ($r>0.95$), thus only one band (near infrared) was used to calculate the texture features. These second order textures measures were considered to be the most relevant texture measures for image classification as well (Baraldi and Parmiggiani 1995).The first and second order texture features are calculated based on formulae shown in Table 3-4. In addition, image statistics were used to explore statistical relationships between texture layers.

In this study, the most feasible window size was estimated for each second order statistics feature using a semivariogram approach (Carr and de Miranda 1998). Determining the spatial extent (i.e. window size) for extracting the GLCM is important for texture analysis, so one of the most common methods for determining window size is based on evaluating the spatial autocorrelation between image pixels. Since semivariogram depicts the relationship between semivariance values (half of the mean of the sum of the square of the difference between pixel values at certain spatial lag distance) and the corresponding lag distances, the semivariance S^2 between a pixel

value z(x) and its neighboring pixel value z(x+h) at a lag distance h were computed as (Carr and de Miranda 1998):

$$S^2 = \frac{1}{2m}\sum_{i=1}^{m}\left[z(x) - z(x+h)\right]^2$$

Where *m* is equal to the number of value pairs in which the separation distance is equal to *h*. The most dominant grass communities in the study area were the Short sawgrass wet prairie (CWP) and Muhlenbergia wet prairie (MWP) (Ross et al. 2003; Ross, Mitchell-Bruker, et al. 2006). The typical diameter of these communities were about 10 meters, thus 30 pixels were included as the range in which semivariance values were calculated for each vegetation class from the training polygons in 8 directions (N, S, W, E, NE, SW, SE, NW).

Separability Analysis

The spectral signatures for this study's five classes were examined visually and statistically. Visual inspection of these signatures indicated strong similarities, except for the Woody vegetation class (Figure 3-3) and can be attributed to within species phenological differences, the relative similarity between involved species and the spatial intermix of plant communities. Examples of such community mix were noted in the existence of Short and Tall sawgrass vegetation within the sawgrass communities and the spatial intermix between the Muhlenbergia wet prairie and Schizachyrium wet prairie classes.

The Jeffries–Matsushita (J–M) separability measure (Richards and Jia 2006) was used to compute the statistical distance between the spectral/textural signatures of each pair of classification classes as represented by their training sets and results were used to determine the optimal classification classes based on the maximum separability

among bands. The J-M separability measure is asymptotic to a value of 2.0. Classes with J-M values close 2.0 imply high separability and thereby providing potentially "good" classification accuracy.

Parametric Classification

In this study, maximum likelihood classifier (ML) classification of different combination of the image spectral information (spectral bands and first and second order texture features) was tested. Maximum likelihood classifier is a statistical classifier that assumes normal distribution for the values of each class' training set and can be described by the mean and covariance matrix. Maximum likelihood uses training areas to compute the distribution statistics from the study areas and use these statistics to calculate the probability of each pixel belonging to a class distribution of values for each spectral band. Maximum likelihood can be calculated by the following discriminant function ($g_i(x)$) for each class:

$$g_i(x) = \ln p(\omega_i) - {}^{1}/_{2} \ln|\Sigma_{\mathrm{i}}| - {}^{1}/_{2} (\chi - m_i)^t \, \Sigma_{\mathrm{i}}^{-1}(\mathrm{x} - \mathrm{m_i})$$

Where i=class, x= data vector, $p(\omega_i)$ = probability that class ω_i occurs in the image and is assumed the same for all classes, Σ_i = covariance matrix of class i, m_i = mean vector of class i and t is the transposition function. The discriminant $g_i(x)$ is calculated for each class and the class with the highest value is selected (Paola and Schowengerdt 1995).

Accuracy Assessment

The classification accuracy was summarized in confusion matrices, where user's, producer's and overall accuracy values were calculated and presented using one third

of the training data set (Table 3-2). User's accuracy as defined in this study measures the probability that a pixel on the map accurately identifies the actual study's vegetation classes. Accuracy was calculated by dividing the total number of correctly classified pixels with the total number of all pixels assigned to that particular class in the map, thus reflecting the measure of commission error. Producer's accuracy measures the probability that a pixel observed in the field is correctly classified in the map and reflects the error of omission, where the correctly classified pixels in a class are divided by total number of pixels of the particular class measured in the field. Overall accuracy is the percentage of correctly classified points from the field data and is computed by dividing the sum of the correctly classified pixels by the sum of all pixels in the error matrix (Congalton 1991; Tso and Mather 2009). In this study, the overall, producer's and user's accuracies of the maps were designated by five standard categories: very high accuracy (over 90%), high accuracy (80%-90%), acceptable accuracy (70%- 80%), low accuracy (50%-70%), and poor accuracy (less than 50%). Additionally, the Kappa coefficient was also used to test whether the generated classification is significantly better than a randomly generated map. Kappa coefficient ranged between 0 and 1, where a 1 indicates total agreement (perfect classification).

Kappa coefficient was calculated as follows:

$$\widehat{K} = \frac{N\sum_{i=1}^{r} x_{ii} - \sum_{i=1}^{r}(x_{i+} \times x_{+i})}{N^2 - \sum_{i=1}^{r}(x_{i+} \times x_{+i})}$$

Where r is the number of rows in the matrix, x_{ii} is the number of observations in row i and column i, x_{i+} and x_{+i} are the marginal totals of row r and column i respectively, and N is the number of observations (Congalton 1991; Foody 2004).

Evaluation of the Classification Results

Kappa coefficients (Foody 2004) were calculated to evaluate the difference between two thematic maps. To compare the kappa coefficients, z-tests were performed to test the hypothesis whether the results of two classifiers are significantly different (Donner et al. 2000) at a 5% level of significance if |z| >1.96 (Congalton 1991).The z-tests were based on the following formula:

$$z = \frac{\widehat{K}_1 - \widehat{K}_2}{(\hat{\sigma}^2_{\widehat{K}_1} + \hat{\sigma}^2_{\widehat{K}_2} - 2\hat{\sigma}_{\widehat{K}_1\widehat{K}_2})}$$

where $\hat{\sigma}_{\widehat{K}_1\widehat{K}_2}$corresponds to the estimated covariance between $\widehat{K}_1$ and $\widehat{K}_2$ (Donner et al. 2000).

Results

Semivariogram Analysis

The spatial autocorrelation of each of the 5 vegetation classes were analyzed to determine optimal window size for texture feature extraction. Spherical semivariograms were calculated using pixel values of the training data sets (Figure 3-4) for each spectral band to estimate the most appropriate window size for the texture features (Figure 3-5). The semivariogram curves of the vegetation classes showed different behaviors in a particular spectral band. However, the semivariogram trends were similar for the classes in a different spectral band. The semivariogram of the Schizachyrium wet prairie (SCWP)' class was the flattest semivariogram with very low semivariance values. The Muhlenbergia WP class had low semivariance values; however its semivariogram was

not as flat as SCWP's, and had rising trend until approximately 3 pixels and was flat with a minor hump at around 11 pixels. The Tall sawgrass marsh had medium semivariance values compared to the other classes with an increasing semivariogram in the first 4-5 pixels, but flattened afterward until 11 pixels and was similar to the Schizachyrium WP class where a minor increase was noticeable. Short sawgrass WP had a shape comparable to the MWP and CM classes with a rising trend in the first 4-5 pixels and low internal variability with a small increase after 10 pixels. The Woody vegetation class had the highest semivariance values and a semivariogram shape that is similar to the MWP, CM and CWP classes showing a clear increasing trend to 4 pixels and low spatial variability afterword. Using these semivariogram curves, the most appropriate window size for extracting the texture features was manually identified. Since most of the classes had very similar patterns with increasing semivariance values up to 4-5 pixels of lag distance followed by a flattened curve, with small variations up to a lag distance of 11 pixels, a set of window sizes ranging between 3 and 15 pixels were tested for the first and second order texture features.

Spectral Separability

Spectral separability analysis using the J-M index revealed that using spectral bands alone would not provide the necessary separability to discriminate among classes (Table 3-5). Only the Woody vegetation class could be classified accurately (J-M > 1.98) if only the four spectral bands were used in the classification. Classes with similar species in the community such as the Short sawgrass wet prairie versus Tall sawgrass marsh had as low J-M value as 0.38. Similarly, Short sawgrass wet prairie versus Muhlenbergia wet prairie had a 0.39 J-M value.

When first and second order textural features were included in the separability analysis, the discrimination accuracy increased (Table 3-6). Most of the class comparisons revealed high separability. Only the Short sawgrass wet prairie and the Muhlenbergia wet prairie had a lower J-M value (1.40). These results indicate the potential of obtaining high classification accuracy by introducing texture features as additional bands in the classification process.

Using Spectral Bands and Normalized Difference Vegetation Index

The ML classifier was implemented (ITT ENVI software) using: (1) the 4 spectral bands only and (2) the spectral bands in combination with the normalized difference vegetation index (NDVI) layer. The classification results (Table 3-7) using the 4 spectral bands resulted in an acceptable overall accuracy (73.8%) and low user's accuracy for the CWP and SCWP classes, while the Woody vegetation class had very high producer's and user's accuracies. When the NDVI layer was included in the ML classification, the overall accuracy of the map increased to 75.4%, which is only a 1.6% improvement in overall accuracy, compared to the accuracy obtained using only spectral bands.

Incorporation of First Order Texture Features

The results using the textural features in addition to the spectral bands are shown in Tables 3-8 and 3-9. Experimenting with different window size used to extract first order texture revealed varying accuracies with the highest overall accuracy (74.08%) was achieved with a 9 by 9 window size (Figure 3-6). The poorest overall accuracy (5.01 %) was achieved for the 5 by 5 window size, which was associated with the very low number of pixels correctly recognized in the CM class. The classified image produced using the 4 spectral bands and their texture features (9 by 9 window) had high

and acceptable accuracies in detecting CWP and MWP classes (81.85% and 75.74%, respectively) with acceptable user's accuracies. The user's accuracy was high for the CM and SCWP classes. When employing larger window size (11 by 11 and 15 by 15) a decreasing trend in overall accuracy was noticeable, this is associated mainly with the poor producer's accuracy of the SCWP class.

Incorporation of Second Order Texture Features

Maximum Likelihood classification results obtained using spectral and second order texture features (using different window sizes) are presented in Tables 3-10 and 3-11. The highest overall accuracy was achieved when a 7 by 7 window was employed (76.89%); however, there was no significant difference between these results ($\alpha>0.05$) and the ones achieved using 5 by 5 window size. However, some of the vegetation communities were classified with higher producer's accuracy using the 3x3 and 9x9 window sizes. For example, the SCWP class had a very high producer's accuracy (89.90%) when using the 3 by 3 window and the CM class had very high producer's accuracy (90.41%) when a 9 by 9 window was employed. When larger windows (e.g. 11 by 11 or 15 by 15) were utilized, the overall accuracy decreased (72.72% and 67.61%, respectively).

Merging Different Window Sizes

The spectral bands and NDVI combination provided a 75.40% overall accuracy (Table 3-7). When texture features from different window sizes were also incorporated in addition to the spectral bands and the NDVI the accuracy of the map significantly increased. Spectral bands, NDVI and first order texture features with the highest overall accuracies(3 by 3 and 9 by 9 pixels windows); were stacked and tested and produced an 81.73% overall accuracy map (Table 3-12). This is significantly better than previous

accuracies obtained using only the spectral bands and NDVI or the spectral bands and only one window size. Moreover, the producer's accuracy increased for all communities except one and the user's accuracy improved or slightly decreased in the case of CM and SCWP classes.

To further reduce the number of bands in the analysis, image statistics were examined for the 3 by 3 and 9 by 9 window first order texture features. The statistics revealed very high correlation (r>0.99) between the 3 by 3 window variance and the 9 by 9 window variance features, while the data range, mean and entropy features for both window sizes were less correlated (r=0.85). Because of the correlation between the variance features, the 3 by 3 pixels window variance and the 9 by 9 pixels window data range, mean and entropy features were merged with the spectral bands and the NDVI layer and classified. The classification results listed in Table 3-12 shows that the overall accuracy increased to 84.01%.

Second order texture features were also tested in combination with the image spectral bands and the NDVI layer. Instead of using the 5 by 5 or 7 by 7 window texture features, which produced the best overall accuracy, the 3 by 3 and 9 by 9 features were used due to their higher producer's and user's accuracy for the SCWP and CM communities (Table 3-10). The overall accuracy using the 3 by 3 and 9 by 9 second order texture features was 84.92%, with very high and high producer's accuracy values for the CM and SCWP classes (94.36% and 87.96%, respectively) and acceptable and low values for CWP (75.35%) and MWP (65.89%) classes. To reduce the number of features, image statistics were reviewed similarly to the first order texture features. The review revealed that the variance feature from the 3 by 3 window was highly correlated

(r>0.94) with the variance feature of the 9 by 9 window variance. Thus, the variance, from the 3 by 3 GLCM and the mean, homogeneity, dissimilarity, entropy and ASM from the 9 by 9 GLCM were used in the classification with the spectral bands and the NDVI layer. The overall accuracy of the classification was 84.33% (Table 3-13), slightly lower than the results obtained using all 3 by 3 and 9 by 9 second order texture features.

Finally, both first and second order texture features (3 by 3 and 9 by 9 window) were utilized with the spectral bands and the NDVI layer. The overall accuracy of the classification was slightly lower (83.97%) compared to the previous results using the first and second order texture features separately (Table 3-13).

Discussion

One of the objectives of this research was to test the performance of the ML classification of wetland communities when texture features were introduced. The results showed that incorporating texture features in the classification yielded better classification accuracy than using the image spectral bands alone. However, when extracted first order texture features using only one window size were included in the analysis, the overall accuracy decreased slightly. The incorporation of the second order texture features extracted from a single window size, slightly increased the achieved overall accuracy. The low overall accuracy associated with using the spectral bands can be explained by the very similar spectral properties of some of the classes as indicated by the J-M separability analysis. For example, the Tall sawgrass marsh (CM), Short sawgrass (CWP) and the Muhlenbergia wet prairie (MWP) classes were poorly detected. The Schizachyrium wet prairie (SCWP) class was incorrectly classified 59.78% of times in the field, had better detection accuracy (76.15%). The inclusion of

the NDVI layer increased the overall accuracy by 1.6% as well as the detectability of the CM, MWP and SCWP classes.

When different window sizes were merged together with the spectral bands and the NDVI layers, the overall accuracy and the accuracy of individual vegetation classes increased significantly ($\alpha<0.05$). This indicates that the additional characteristics of the texture features developed from multiple window size provide useful information, which can improve the accuracy of the automated classification algorithm. Results from similar studies indicated similar findings when spectral bands and different window sizes were included in the analysis (Wulder et al. 1998; Johansen et al. 2007; Dillabaugh and King 2008; Barbosa 2010). Johansen et al. (2007) as well as Barbosa (2010) achieved 78.95% and over 80% overall accuracy when classifying wetland vegetation, respectively, when using both spectral bands and texture features (contrast, dissimilarity, homogeneity, ASM. Dillabaugh and King (2008) reached 88% overall accuracy when classifying broad wetland classes (marsh, floating aquatic, emergent aquatic, forest, open water).

The window size was an important parameter when deriving texture measures. The window size is associated with the scale of the image content as expressed by individual objects. In this study, the objects were individual plant community elements that can be differentiated from a certain sized area relative to the image's spatial resolution. The communities included not only larger contiguous areas (CM class), but also smaller discontinuous patches such as the Schizachyrium wet prairie. Moving windows between 3 by 3 and 15 by 15 pixels were tested considering the smallest vegetation patches in the area, image resolution, and the range property of the

semivariogram. The results indicated that in the case of the CM class, which can cover larger areas, small window size (3 by 3 window) was not appropriate (producer's accuracy is 12.56%). Similar findings can be inferred for the MWP class. The producer's accuracy of both classes increased, in the case of CM class from 12.56% (3 by 3 window) to 70.33% (9 by 9 window), while the Woody vegetation class' detection rate was similar regardless of the size of the moving window. The CWP class classification accuracy showed some variations with different window sizes but remained above 63% except when a 7 by 7 window size was used (producer's accuracy decreased to 42.5%).

The SCWP class showed a decreasing trend in producer's accuracy when the window size was increased. When small window size (3 by 3) was tested, the SCWP class reached 89.90% producer's accuracy with an overall accuracy of 70.46%. Larger window sizes (5 by 5 and 7 by 7) produced almost identical overall accuracy (76.35% vs. 76.89%); however, the accuracy of the SCWP class started to decrease, when 9 by 9 or larger window size was used. This increase in window size (9 by 9 and more) was associated with an increase in the CM class accuracy, which reached a 90.41% producer's accuracy. Short sawgrass and the MWP class accuracy were steady in all window sizes indicating insensitivity to window size. Overall, accuracy declined significantly when window size was increased above 9 by 9 for all classes indicating that larger window sizes are not appropriate in detecting small-size vegetation communities in the ENP. This highlights the importance of determining the best window size (or combination of windows), where optimal classification accuracy of different vegetation communities can be achieved.

Texture features obtained from different window sizes, that best facilitated the delineation of the vegetation communities were merged and examined. Since the Woody vegetation, CWP, MWP classes were less sensitive to window size changes and the 3 by 3 and 9 by 9 window sizes helped in best delineating the SCWP and CM classes, these window sizes were used in the analysis with the spectral bands and the NDVI layer. When 3 by 3 and 9 by 9 first order texture features were used, the overall accuracy increased significantly ($\alpha<0.05$) compared to either using the spectral bands only (73.80% vs. 84.01%), or using texture features from a single window size (76.89% vs. 84.01%). Since, the SCWP class had very high producer's accuracy when the 3 by 3 window size was used, its variance feature was merged with the 9 by 9 window range, mean and entropy features as well as the spectral bands and the NDVI layer. The overall accuracy of this combination increased significantly to 84.01% ($\alpha<0.05$) compared to the spectral bands, NDVI, and all available (3 by 3 and 9 by 9) first order texture features (81.73%). This implies that variance feature is a very important feature for differentiating among classes and furthermore when decreasing the number of layers in the classification and the results are statistically different ($\alpha<0.05$); the computation time was reduced. Second order texture, 3 by 3, and 9 by 9 features were also merged with the spectral bands and NDVI and this resulted in an 84.92% overall accuracy. Similar to the first order texture features, the 3 by 3 variance and the 9 by 9 mean, homogeneity, dissimilarity, entropy and ASM were tested and resulted in a slightly decreased overall accuracy (84.33%).

This study's results indicate that a combination of first and second order texture features and different moving window sizes in addition to the image spectral bands and

NDVI layer perform significantly better ($\alpha<0.05$) than all other data combinations. In general, first order texture features are easier to compute and the classifier tends to be faster because of the less number of features (data range, mean, variance and entropy) compared to the second order texture features, which are more computationally exhaustive and have more features to include in the classification. The best window size depends on the spatial distribution of a particular vegetation class. For example, the SCWP class was differentiated very well with smaller window size, while the CM class needed a larger window size. This observation agrees with previous work (Ouma et al. 2008), which showed that the most appropriate texture feature and window size(s) to classify a vegetation community depend on the textural pattern of this particular vegetation community. The semivariogram analysis was found to be useful for estimating the spatial autocorrelation within the vegetation communities, and hence defining a range of window sizes to extract texture features. However, it did not specify the preferred window size for each class. A large window size can depict the spatial patterns of large-patches communities; however when delineating vegetation communities of smaller patches, larger window sizes can capture additional communities and increase the overall error rate. To correct for this, windows should be small enough for communities of small spatial extent so as to keep the variability low and to maximize the potential for class separability.

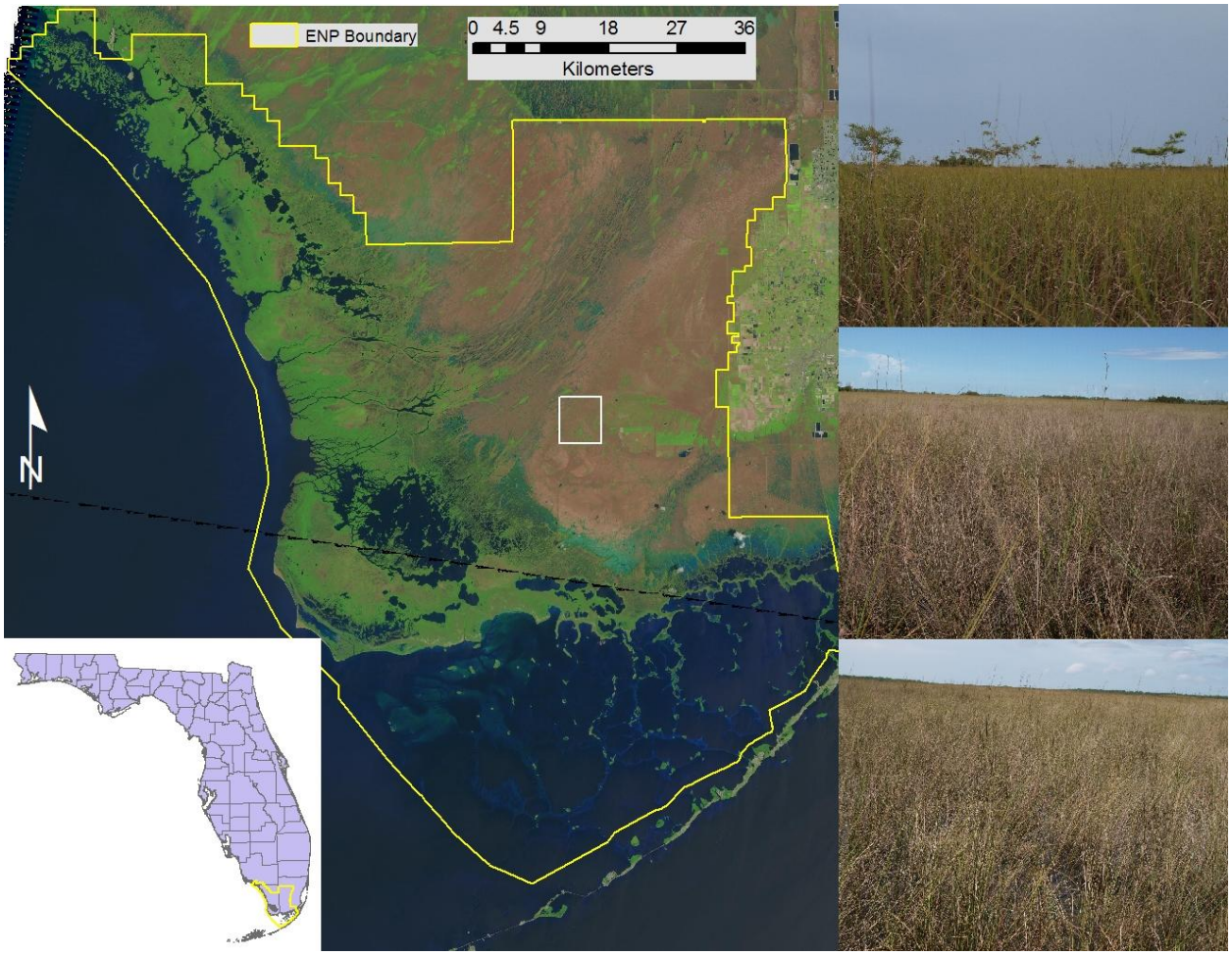

Figure 3-1. Location of study area in the Everglades National Park based on a Landsat Thematic Mapper 5 image in true color composite. The images to the right show Short sawgrass wet prairie with some trees (top), Muhlenbergia wet prairie (middle) and Schizachyrium wet prairie (bottom).

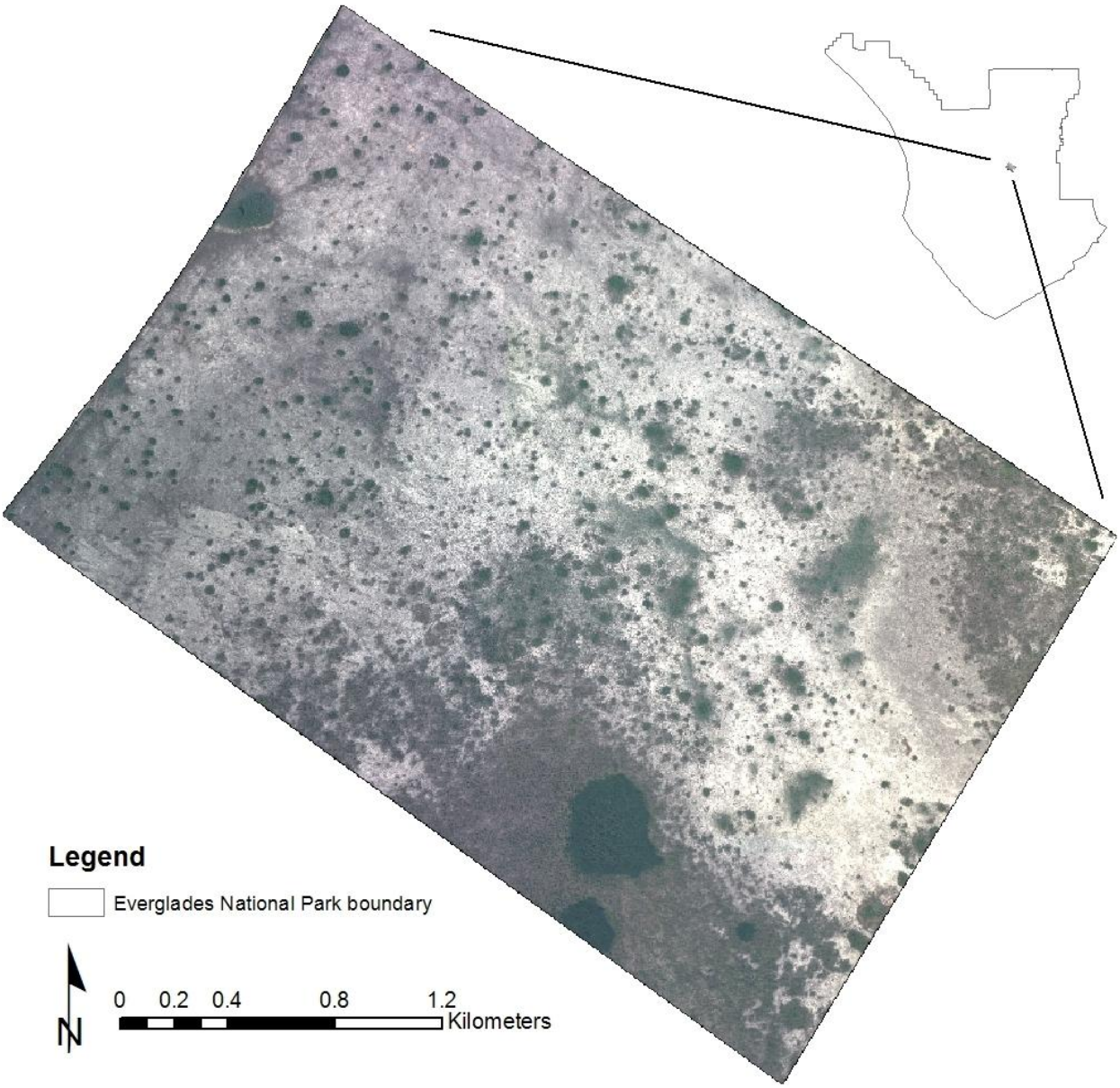

Figure 3-2. Microsoft Vexcel UltacamX mosaiced image covering the study area in the ENP.

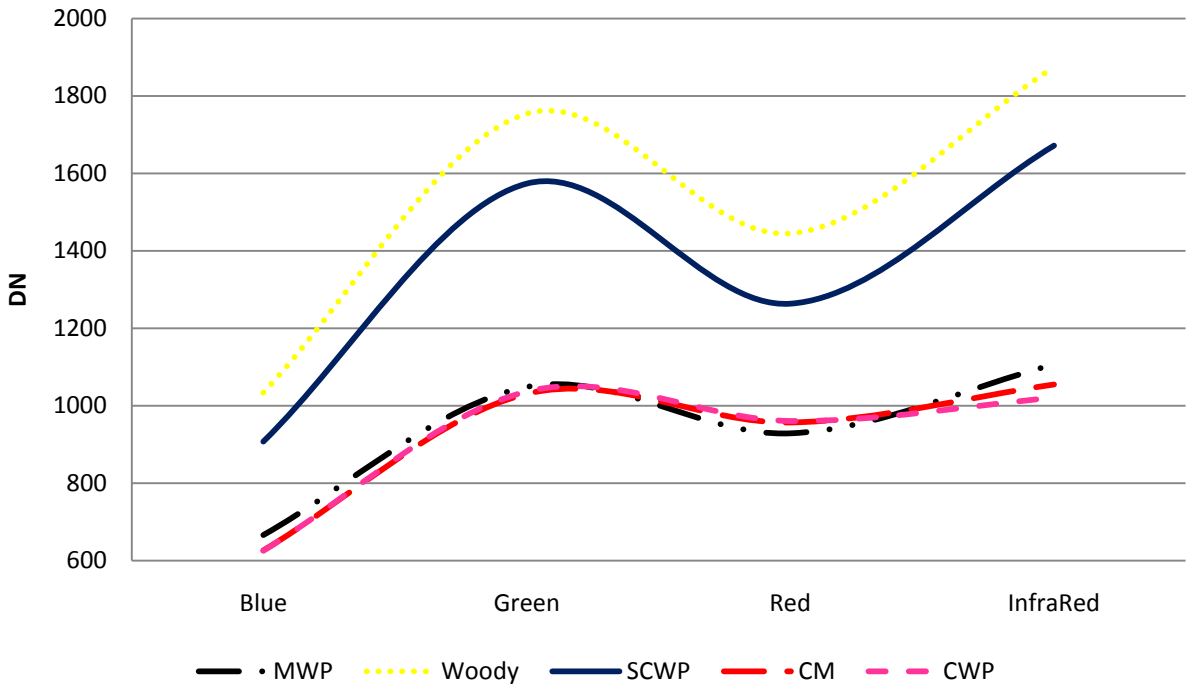

Figure 3-3. Spectral response curve for the studied vegetation communities in the Blue. Green, Red and Infrared spectral bands. DN - Digital Numbers. CM - Tall sawgrass marsh, CWP - Short sawgrass wet prairie, MWP - Muhlenbergia wet prairie, SCWP - Schizachyrium wet prairie, Woody - Woody vegetation.

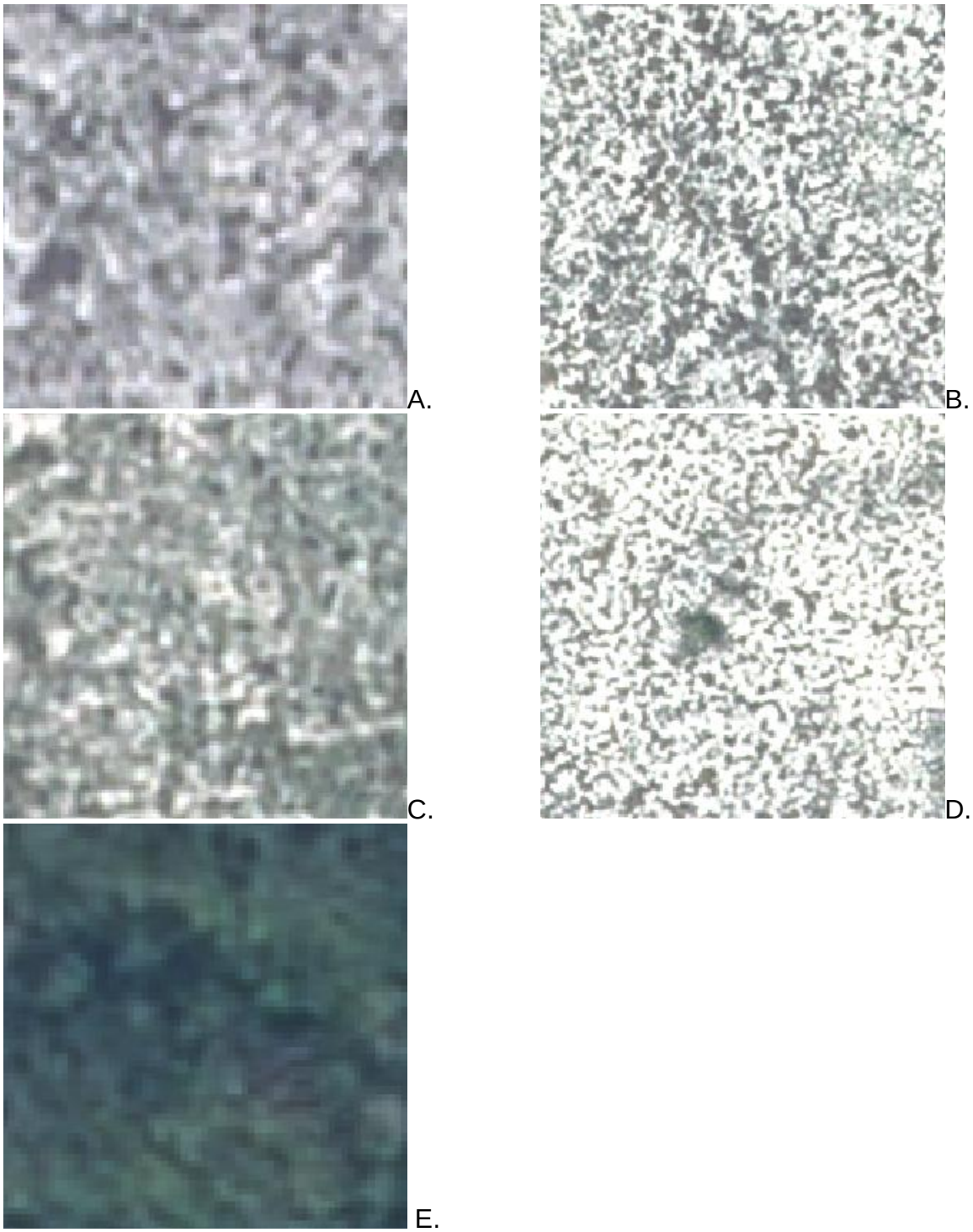

Figure 3-4. Selected training sites for semivariance calculation. (A) - Schizachyrium wet prairie, (B) - Muhlenbergia wet prairie, (C) - Tall sawgrass marsh, (D) - Short sawgrass wet prairie, (E) - Woody vegetation.

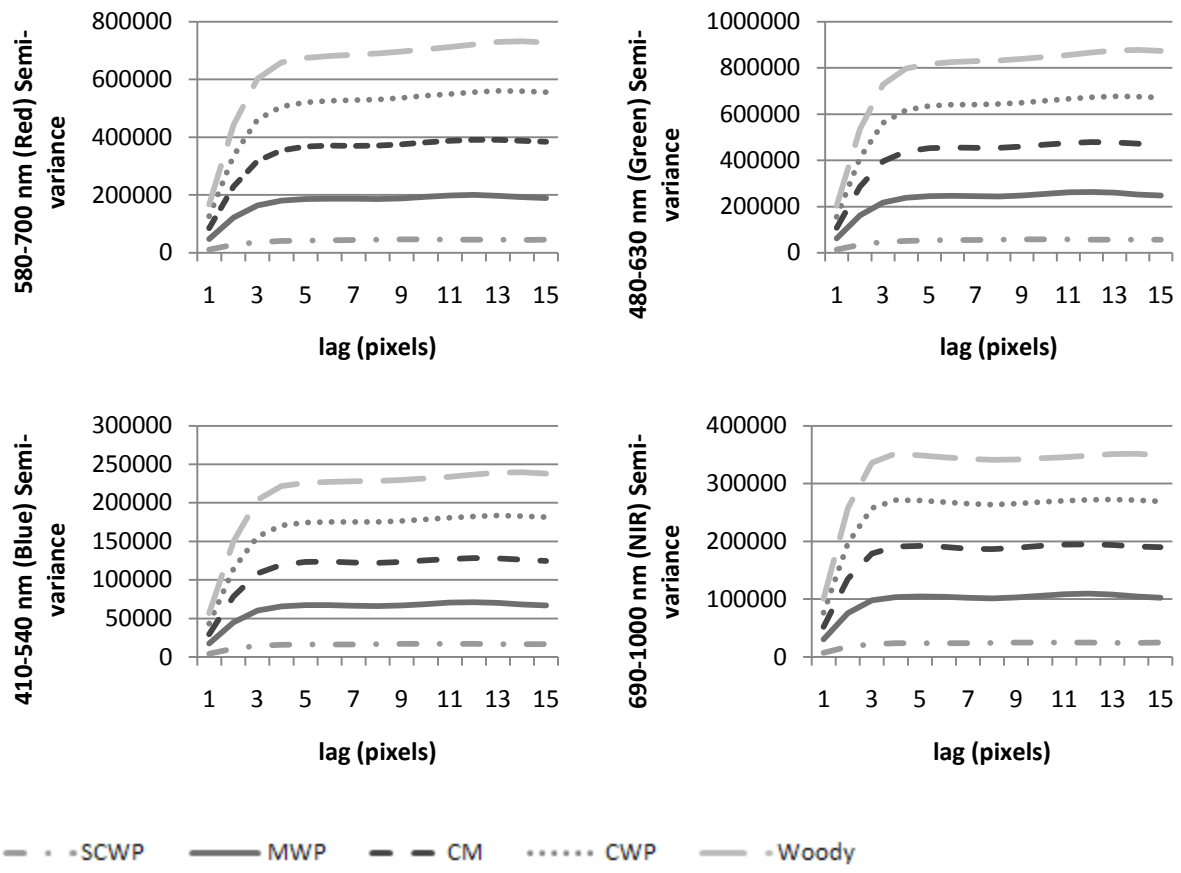

Figure 3-5. Semivariograms derived from four spectral bands for the selected training sites. CM - Tall sawgrass marsh, CWP - Short sawgrass wet prairie, MWP - Muhlenbergia wet prairie, SCWP - Schizachyrium wet prairie, Woody - Woody vegetation.

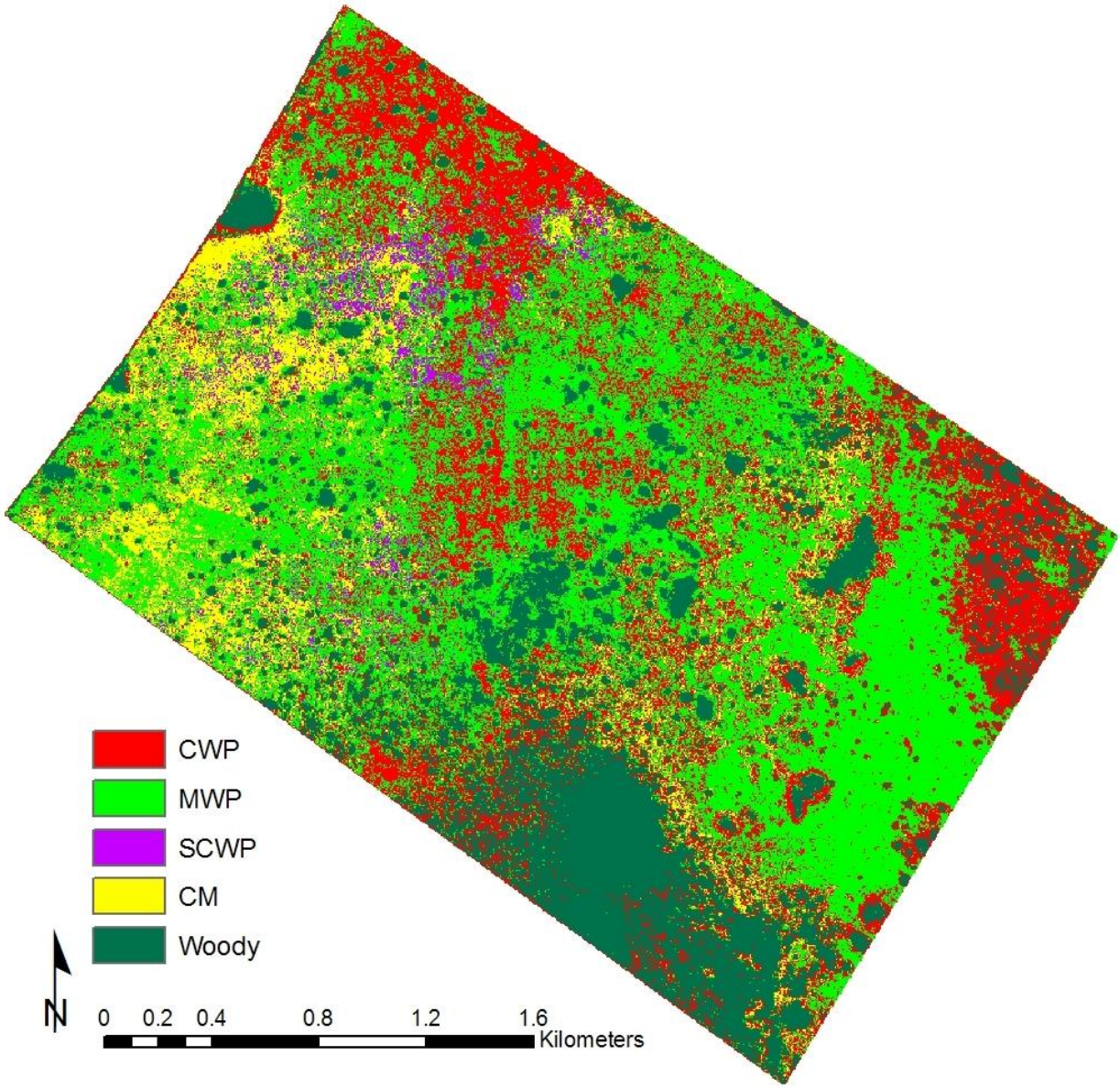

Figure 3-6. Land cover map based on spectral bands, Normalized Difference Vegetation Index layer and first order texture features (3 by 3 window variance and 9 by 9 window data range, mean, entropy). CM - Tall sawgrass marsh, CWP - Short sawgrass wet prairie, MWP - Muhlenbergia wet prairie, SCWP - Schizachyrium wet prairie, Woody - Woody vegetation.

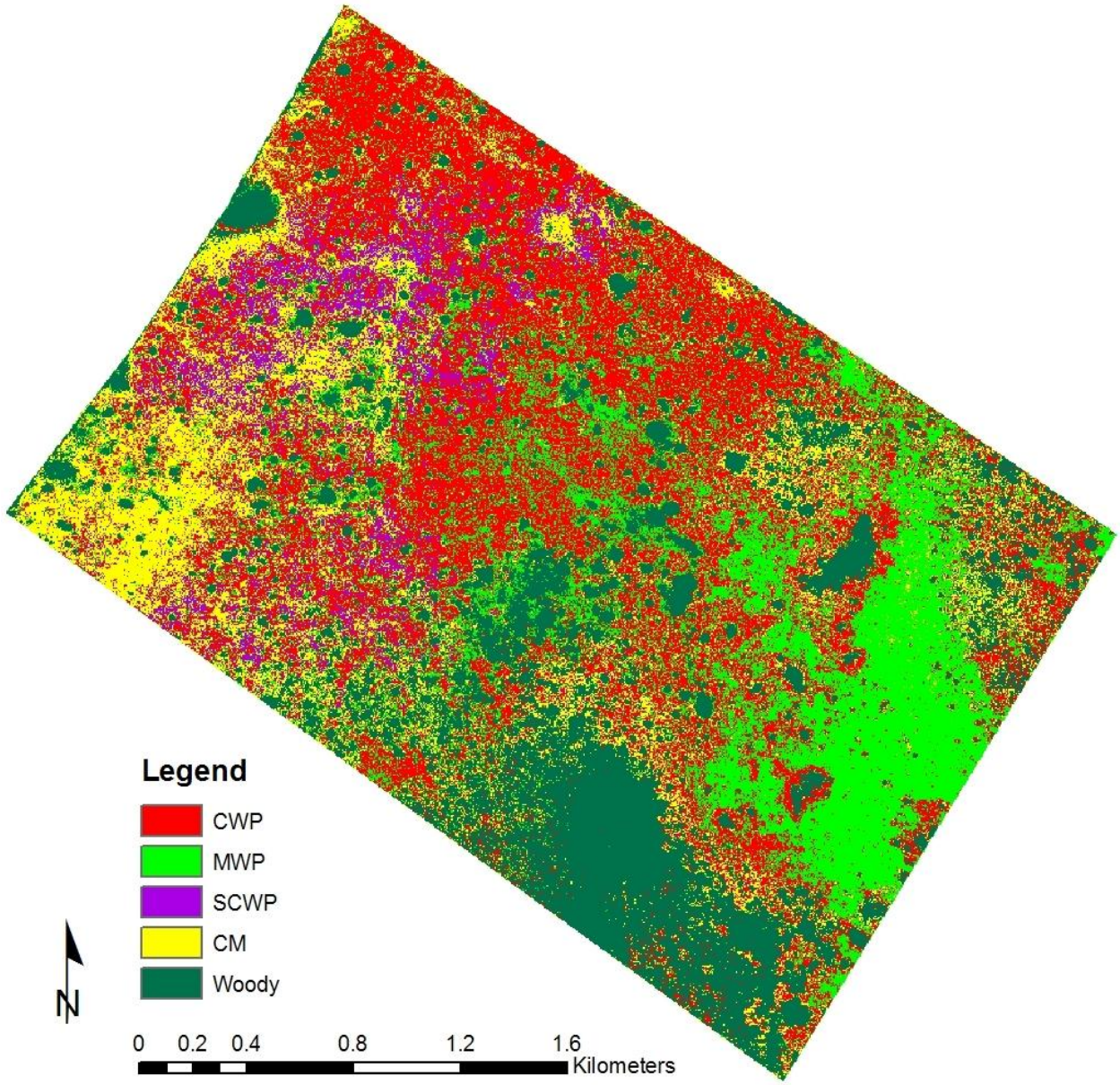

Figure 3-7. Land cover map based on spectral bands, NDVI layer and second order texture features (3 by 3 and 9 by 9 window). CM - Tall sawgrass marsh, CWP - Short sawgrass wet prairie, MWP - Muhlenbergia wet prairie, SCWP - Schizachyrium wet prairie, Woody - Woody vegetation.

Table 3-1. Major plant communities in the study area modified from Ross et al. (2003 and 2006) and Richardson et al. (2008).

Class name	Dominant plant species
Tall sawgrass marsh (CM)	Dominated by dense, tall stands of *Cladium jamaicense,* some *Eleocharis cellulosa* and *Typha domengensis* Pers.
Short sawgrass wet prairie (CWP)	Moderate stands of *Cladium jamaicense* (<22%), and some *Rhynchospora* spp., *Schoenus nigricans,* May also have *Schizachyrium rhizomatum*
Schizachyrium wet prairie (SCWP)	*Schizachyrium rhizomatum* and some sparse/moderate stands of short *Cladium jamaicense*
Muhlenbergia wet prairie (MWP)	Mix of *Muhlenbergia capillaries, Cladium jamaicense Schizachyrium rhizomatum,* and some *Schoenus nigricans*
Woody vegetation (Woody)	Dominated by *Salix caroliniana, Persea borbonia, Magnolia virginiana*

Table 3-2. Description of collected ground reference data.

Classes	Number of points collected	Number of pixels selected for training set	Number of pixels selected for accuracy testing	Average number of pixels in a training and accuracy polygon
CM	48	12536	3237	328
CWP	60	14733	4730	324
SCWP	36	12782	3856	462
MWP	56	12940	3737	297
Woody	56	13439	4685	323

CM - Tall sawgrass marsh, CWP - Short sawgrass wet prairie, MWP - Muhlenbergia wet prairie, SCWP - Schizachyrium wet prairie, Woody - Woody vegetation.

Table 3-3. Aerial imagery data characteristics.

Sensor	Microsoft Vexcel UltracamX
Acquisition date	March 28 – April 10, 2009
Flight altitude	4115 ± 90 meter
Spectral resolution	Red (580 …. 700 nanometer) Green (480 …. 630 nanometer) Blue (410 …. 570 nanometer) Near Infrared (690 …. 1000 nanometer)
Spatial resolution	0.305 meter
Data	Spectral Bands Derived Texture Features
Radiometric resolution	14 bit
Area covered by one image	4400 m x 2870
Overlap	60% forward lap 40% side lap

Table 3-4. Texture feature calculation formulae.

Feature	Formula
First order statistics*	
Data range	$\max\left(z_{ij}\right) - \min\left(z_{ij}\right)$
Mean (μ)	$\frac{\sum z_{ij}}{n}$
Variance (v)	$\frac{\sum (z_{ij} - \mu)^2}{n-1}$
Entropy	$-\sum_{i} P(i) \log P(i)$
Second order statistics**	
Mean	$\sum_{\mathrm{i}} \sum_{\mathrm{j}} P(i,j)/n$
Variance	$\sum_{\mathrm{i}} \sum_{\mathrm{j}} (i-\mu)^2 P(i,j)$
Homogeneity	$\sum_{i} \sum_{j} \frac{1}{1+(i-j)^2} P(i,j)$
Dissimilarity	$\sum_{i} \sum_{j} \lvert i-j \rvert P(i,j)$
Entropy	$-\sum_{i} \sum_{j} P(i,j) \log P(i,j)$
Angular second moment	$\sum_{i} \sum_{j} P^2(i,j)$

* Where z_{ij}= grey level of the pixel, n = number of pixels in a window and $P(i)$ = is the probability that the difference between two adjacent pixels is equal to i (Irons and Petersen 1981; Culbert et al. 2009).
** Where $P(i,j)$ is the (i,j)th entry in the co-occurrence matrix (Haralick et al. 1973).

Table 3-5. Jeffries-Matsushita (J-M) separability analysis using the 4 spectral bands.

Classes	J-M value
CWP and CM	0.38
CWP and MWP	0.39
MWP and CM	0.66
SCWP and CM	0.84
CWP and SCWP	1.02
MWP and SCWP	1.20
MWP and Woody	1.98
CM and Woody	1.99
CWP and Woody	1.99
SCWP and Woody	1.99

CM - Tall sawgrass marsh, CWP - Short sawgrass wet prairie, MWP - Muhlenbergia wet prairie, SCWP - Schizachyrium wet prairie, Woody - Woody vegetation.

Table 3-6. Jeffries-Matsushita (J-M) separability analysis using the 4 spectral bands, first and second order texture features.

Classes	J-M value
CWP and MWP	1.40
CWP and CM	1.89
SCWP and CM	1.92
MWP and CM	1.95
CWP and SCWP	1.98
MWP and SCWP	1.99

CM - Tall sawgrass marsh, CWP - Short sawgrass wet prairie, MWP - Muhlenbergia wet prairie, SCWP - Schizachyrium wet prairie, Woody - Woody vegetation.

Table 3-7. Maximum likelihood classification results using spectral bands and Normalized Difference Vegetation Index (NDVI) layer.

Class	Spectral bands		Spectral bands and NDVI layer	
	PA	UA	PA	UA
CM	52.46	73.49	63.80	77.65
CWP	63.57	62.17	52.98	74.19
MWP	70.85	74.20	71.31	71.60
SCWP	76.15	59.78	83.69	58.44
Woody	100.00	100.00	100.00	100.00
Overall accuracy (%)	73.8070		75.4016	
Kappa Coefficient	0.6716		0.6915	

PA - Producer's accuracy(%), UA - User's accuracy(%), CM - Tall sawgrass marsh, CWP - Short sawgrass prairie, MWP - Muhlenbergia wet prairie, SCWP - Schizachyrium wet prairie, Woody - Woody vegetation. Kappa value closer to 1 means better map accuracy.

Table 3-8. Maximum likelihood classification results for spectral bands and first order texture features with different window sizes.

Class	SB + first order texture 3x3		SB + first order texture 5x5		SB + first order texture 7x7		SB + first order texture 9x9	
	PA	UA	PA	UA	PA	UA	PA	UA
CM	12.56	93.61	5.01	100.00	63.93	91.94	70.33	79.92
CWP	79.30	53.92	62.93	58.98	42.50	74.39	81.85	57.03
MWP	70.09	82.53	80.64	44.04	86.03	44.65	75.74	62.63
SCWP	78.78	53.96	61.46	65.03	56.29	74.37	39.75	81.96
Woody	100.00	100.00	100.00	100.00	99.97	100.00	99.92	100.00
Overall accuracy (%)	70.1313		64.2338		70.7938		74.0884	
Kappa Coefficient	0.6247		0.5501		0.6336		0.6758	

SB - Spectral bands, PA - Producer's accuracy(%), UA - User's accuracy(%), CM - Tall sawgrass marsh, CWP - Short sawgrass wet prairie, MWP - Muhlenbergia wet prairie, SCWP - Schizachyrium wet prairie, Woody - Woody vegetation.

Table 3-9. Maximum likelihood classification results for spectral bands and first order texture features with different window sizes.

Class	SB + first order texture 11 by 11		SB + first order texture 15x15	
	PA	UA	PA	UA
CM	68.88	76.21	70.85	66.29
CWP	65.03	69.89	65.94	61.93
MWP	84.87	48.88	83.50	52.24
SCWP	36.03	85.07	26.30	90.92
Woody	99.82	100.00	99.69	100.00
Overall accuracy (%)	71.6379		69.8851	
Kappa Coefficient	0.6448		0.6233	

SB - Spectral bands, PA - Producer's accuracy(%), UA - User's accuracy(%), CM - Tall sawgrass marsh, CWP - Short sawgrass wet prairie, MWP - Muhlenbergia wet prairie, SCWP - Schizachyrium wet prairie, Woody - Woody vegetation.

Table 3-10. Maximum likelihood classification results for spectral bands and second order texture features with small Grey-Level Co-occurrence Matrix.

Class	SB + second order texture 3x3		SB + second order texture 5x5		SB + second order texture 7x7		SB + second order texture 9x9	
	PA	UA	PA	UA	PA	UA	PA	UA
CM	36.12	66.24	68.82	72.04	85.65	71.26	90.41	66.06
CWP	59.20	80.72	68.53	80.21	66.77	76.20	69.31	70.44
MWP	54.76	64.70	56.81	65.50	59.71	61.97	61.67	60.75
SCWP	89.90	55.81	81.22	68.98	70.24	76.05	51.60	78.42
Woody	99.96	91.62	100.00	91.60	100.00	93.93	100.00	93.55
Overall accuracy (%)	70.4646		76.3511		76.8963		74.3284	
Kappa Coefficient	0.6264		0.7026		0.7107		0.6796	

SB - Spectral bands, PA - Producer's accuracy(%), UA - User's accuracy(%), CM - Tall sawgrass marsh, CWP - Short sawgrass wet prairie, MWP - Muhlenbergia wet prairie, SCWP - Schizachyrium wet prairie, Woody - Woody vegetation.

Table 3-11. Maximum likelihood classification results for spectral bands and second order texture features with large Grey-Level Co-occurrence Matrix (11 by 11 and 15 by 15).

Class	SB + second order texture 11x11		SB + second order texture 15x15	
	PA	UA	PA	UA
CM	89.99	65.19	72.09	62.90
CWP	71.18	68.05	72.59	50.67
MWP	63.76	57.51	66.16	55.02
SCWP	41.70	80.93	29.65	86.61
Woody	99.86	92.92	99.79	99.29
Overall accuracy (%)	72.7244		67.6122	
Kappa Coefficient	0.6601		0.5966	

SB - Spectral bands, PA - Producer's accuracy(%), UA - User's accuracy(%), CM - Tall sawgrass marsh, CWP - Short sawgrass wet prairie, MWP - Muhlenbergia wet prairie, SCWP - Schizachyrium wet prairie, Woody - Woody vegetation.

Table 3-12. Maximum likelihood classification results for spectral bands and first order texture features with merged window sizes.

Class	SB + first order texture 3x3 and 9x9		SB + first order textural features 3 by 3 variance and 9 by 9 data range, mean, entropy	
	PA	UA	PA	UA
CM	88.14	75.53	90.31	79.23
CWP	62.63	87.42	70.22	84.39
MWP	72.71	65.94	72.77	78.79
SCWP	88.14	75.53	85.08	76.45
Woody	100.00	100.00	100.00	100.00
Overall accuracy (%)	81.7329		84.0192	
Kappa Coefficient	0.7712		0.8000	

SB - Spectral bands, PA - Producer's accuracy(%), UA - User's accuracy(%), CM - Tall sawgrass marsh, CWP - Short sawgrass wet prairie, MWP - Muhlenbergia wet prairie, SCWP - Schizachyrium wet prairie, Woody - Woody vegetation.

Table 3-13. Maximum likelihood classification results for spectral bands and first and second order texture features with merged window sizes.

Class	SB + second order texture 3x3 and 9x9		SB + second order texture 3x3 variance and 9x9 mean, homogeneity, dissimilarity, entropy and ASM		SB + 1st and 2nd order 3 by 3 and 9 by 9 window	
	PA	UA	PA	UA	PA	UA
CM	94.36	86.60	87.57	91.90	95.85	84.41
CWP	75.35	81.75	68.21	83.31	71.83	81.98
MWP	65.89	77.93	68.43	73.28	69.21	75.75
SCWP	87.96	76.54	93.48	73.08	83.78	77.24
Woody	99.97	100.00	100.00	100.00	100.00	100.00
Overall accuracy (%)	84.9279		84.3358		83.9782	
Kappa Coefficient	0.8114		0.8040		0.7993	

SB - Spectral bands, PA - Producer's accuracy(%), UA - User's accuracy(%), CM - Tall sawgrass marsh, CWP - Short sawgrass wet prairie, MWP - Muhlenbergia wet prairie, SCWP - Schizachyrium wet prairie, Woody - Woody vegetation.

CHAPTER 4
CLASSIFICATION OF WETLAND COMMUNITIES: USING HIGH RESOLUTION AERIAL IMAGERY AND TESTING ALGORYTHMS

Introduction

Wetlands are an essential part of the global ecosystem since they provide habitat for endangered species, supply groundwater aquifers with water and can reduce floods (Mitsch and Gosselink 2007). In recent years, the growth of urban areas combined with intense agriculture and drainage canals has detrimentally disturbed and polluted the Everglades ecosystem (Junk et al. 2006; Marella 2009; Richardson 2010). The Everglades restoration program is in progress (Comprehensive Everglades Restoration Plan - CERP), and its main task is to develop a method to better capture fresh water and convey it to areas where water is scarce before it enters the Atlantic Ocean and Florida Bay. The transferred water will be used to revitalize the ecosystem, help agriculture, and provide an additional drinking water source for south Florida.

Freshwater sawgrass marsh and wet prairies cover about 44% of the Everglades (Davis et al. 1994). Sawgrass marshes are characterized by an abundance of *Cladium jamaicense* or are sometimes mixed with other species such as *Eleocharis cellulosa* and *Typha domengensis* (Richardson 2010). Wet prairies consist of four major types of grasses: *Schizachyrium* spp., *Muhlenbergia* spp., *Schoenus* spp., and *Cladium* spp. (Olmsted and Armentano 1997), and are named after their dominant species. However, wet prairies also support a high diversity of other plant species (Davis et al. 2005).

Sawgrass marshes and wet prairies are continuously changing and shifting due to several factors such as longer dry seasons, loss of organic soils, increased fire frequency, spread of Woody vegetation and non-native and exotic species (Gunderson 1997; Childers et al. 2003; Zweig and Kitchens 2008; Larsen et al. 2011). Continuous

and frequent monitoring of these areas is necessary to better understand changes in their size, distribution and composition (Olmsted and Armentano 1997). According to Armentano et al. (2006) these grass communities will be the first to change in response to the CERP restoration process, sea level rise, climate change or inputs of chemical fertilizers or pollutants. In addition, it is important to predict changes to flora and fauna habitat to more effectively prevent further degradation of these communities. (Armentano et al. 2006) predicted that observable change in prairie and marsh vegetation in the Everglades National Park (ENP) may occur every few years.

Accurate and timely mapping of wetlands is a major interest of many remote sensing professionals, land managers and decision-makers (Ozesmi and Bauer 2002). However, most of the existing researches consist of delineating and discriminating wetlands from other type of land cover using medium or high resolution imagery (Baker et al. 2006; Nielsen et al. 2008) and differentiating between major plant communities such as grassland vs. forested wetlands (Kindscher et al. 1997; Johansen et al. 2007; Maxa and Bolstad 2009; Bwangoy et al. 2010). Very few studies have attempted to map vegetation communities of small extent (Harvey and Hill 2001; Gilmore et al. 2008; Barbosa 2010), because of the lack of availability of high resolution satellite and aerial imagery.

Recent effort to classify and map vegetation communities in the ENP was conducted in the late 1990's and used direct photo-interpretation of 1:40,000-scale color infrared (CIR) film-based vertical aerial photographs taken in the mid-1990's (Madden et al. 1999). The ENP conducted a field survey in 2007 to assess the accuracy of

Madden's et al. (1999) mapping effort and found significant changes and differences in the present vegetation regime compared to the existing map.

Ozesmi and Bauer (2002) reviewed most of the literature on satellite remote sensing and found that the main problem in wetland remote sensing is the spectral separability of vegetation. Schmidt and Skidmore (2003) also recognized that mapping major physiognomic or forest type classes was fairly straightforward with good accuracy results, but differentiation among grasses or sedges was difficult. The authors also concluded in their review that identification of wetland types at a medium spatial resolution was complicated, and because of the temporal characteristics of most satellites, it was difficult to capture optimal lighting and water level conditions. As a result, high resolution aerial photography is preferred for more detailed and accurate wetland mapping.

Visual photo interpretation has been used in several wetland mapping studies (Madden et al. 1999; Rutchey et al. 2008; Maxa and Bolstad 2009) with good overall accuracy results. However it is extremely costly in terms of time and labor, and moreover, highly depends on the photo interpreter’s skills and knowledge of the area (Ozesmi and Bauer 2002). Baker et al. (2006) conversely found that multispectral image classification of wetlands has similar accuracy and is more repeatable relative to human photo- interpretation. Studies have shown that automated remote sensing techniques such as Maximum-Likelihood (ML), Decision Trees (DT) and Artificial Neural Networks (ANN) (Wang et al. 2004; Baker et al. 2006; Belluco et al. 2006; Wright and Gallant 2007; Sesnie et al. 2008) are effective alternatives to photo-interpretation for mapping wetlands.

Decision trees and ANNs to a lesser extent have become popular recently because they make no assumption about the statistical distribution of the data (Richards and Jia 2006). Decision tree classifiers have been used to successfully partition the input data into more numerous and homogeneous subsets by producing optimal rules which minimize the error rates in the branches of the tree (Friedl and Brodley 1997; Pal and Mather 2003; Yang et al. 2003). In addition, DTs provide a more comprehensive understanding of relationships between objects at different scales of observation or at different levels of detail. The two methods for conducting a decision based classification are manual (Swain and Hauska 1977) and utilization of existing data mining algorithms that are based on different statistical methods that organize incoming data (i.e. Chi-squared Automatic Interaction Detector – CHAID (Kass 1980), Classification and Regression Trees – CART (Breiman et al. 1984), C5.0 (Quinlan 1993), Quick, Unbiased, Efficient Statistical Tree – QUEST (Loh and Shih 1997). Most algorithms are available commercially as standalone applications or built into statistical software products (CHAID, CART, C5.0). The QUEST algorithm is easily accessible and free of charge.

Artificial Neural Networks have been reported to perform more accurately than other techniques (Goel et al. 2003; Mas and Flores 2008) for remotely sensed imagery classification, especially when the feature space is complex or the datasets have different statistical distributions. Thus, when additional data beside band information is incorporated (Benediktsson et al. 1993), ANN might perform better than statistical classification techniques. Moreover, ANNs perform supervised classification using less training data than the ML because the rules of recognition of a category are based on

the characteristics not only of the training data of this particular category class but also of the other classes (Paola and Schowengerdt 1995). The most commonly used ANN in land cover classification studies is the multi-layer perceptron (MLP) neural network based on back propagation (BP) algorithm (Benediktsson et al. 1993; Paola and Schowengerdt 1995; Ghedira et al. 2000; Lloyd et al. 2004; Mas 2004; Fuller 2005; Berberoglu et al. 2007).

(Ozesmi and Bauer 2002) noted that in most cases, improved classification was obtained when using automated techniques such as ML, DT, ANN methods, and incorporating image texture information and multispectral data in the analysis (Ghedira et al. 2000; Wang et al. 2004; Fuller 2005; Wright and Gallant 2007). Wang et al. (2004) incorporated first and second order texture features into their ML classification model, and their results indicated that texture increased the classifier's accuracy significantly when using a 21 by 21 window size. Wright and Gallant (2007) tried to discriminate five palustrine wetland types and when image texture features, DEMs and other ancillary GIS data were added to the multispectral data: the overall average error rate was reduced incrementally. However, Michishita et al. (2008) compared a decision tree classifier with ancillary (i.e. DEM and land surface temperature and other spectral indices) data against the ML classifier at the wetland plant family level and found that ML performed slightly better than the DT. Artificial neural networks are also used in landcover mapping (Paola and Schowengerdt 1995; Berberoglu et al. 2007; Ashish et al. 2009) frequently, but literature on wetland mapping using ANNs is limited (Ghedira et al. 2000; Mas 2004; Fuller 2005).

These previous studies demonstrated that ANN can be used to improve vegetation discrimination. However, accuracy results involving texture features in the analysis vary. In a recent land-use classification study Ashish et al. (2009) employed probabilistic ANN where 1 meter resolution multispectral image and second order texture features (Haralick et al. 1973) were included in the classification process. The overall accuracy, when image texture was included in the analysis was 89%. Berberoglu et al. (2007) tested several texture features for landcover mapping with ML and ANN classifiers and found that ANN outperformed the ML classifier without texture data in the overall classification accuracy when using Landsat spectral bands. The ANN also performed better when texture data was incorporated into the classification; however the overall accuracy slightly decreased when classifying agricultural and semi-natural land covers. Ghedira et al. (2000) attempted to distinguish between wetland categories using ANN and texture information with RadarSat data and concluded that an ANN back propagation algorithm is an accurate tool for image classification. When texture was included in their analysis, the classification process improved significantly. Mas (2004) used Landsat imagery to map land cover classes in a tropical coastal area and employed ANN and ancillary data such as elevation and soil data into his model. When the output from that model was compared with an output from spectral classification, a significant increase of accuracy of land use classification (from 67% to 79%) was detected. Finally, multispectral IKONOS imagery was used in Fuller's (2005) study to detect invasive Melaleuca trees, sawgrass, and 3 other vegetation classes in South Florida. Back propagation ANN was employed using input layers consisting of the spectral bands as well as a texture layer and normalized difference vegetation index.

The author achieved over 85% in overall accuracy, however visual inspection revealed that a class called “other woody type” was frequently misclassified as Melaleuca class.

Overall, most of the previously mentioned studies were generally based on satellite or hyperspectral imagery and used high to low spatial resolution data. Additionally, delineation of wetlands from other land cover types was frequently the main objectives, rather than delineating wetland and grassland classes or species. As a result, there is a need to develop a new vegetation community map for the ENP using rapid and cost effective mapping techniques. Thus the specific objectives of this study are to:

1. Determine whether decision tree and artificial neural network technologies can be applied accurately to delineate among the dominant graminoid/sedge communities in the ENP using high resolution aerial imagery and texture data.
2. Develop a methodology that can be utilized in change detection studies in the Everglades or other wetlands using high resolution imagery and texture data. Results can be used to rapidly monitor and assess changes in wetland vegetation communities.

Methods

Study Area

The 8.5 km² study area is located within the Everglades National Park at 25º25´09.09´´ to 25º24´15.16´´ N and 80º46´41.46´´ to 80º45´41.00´´ W (Figure 4-1) and is composed of mostly graminoid and sedge communities with some woody vegetation present as well. The most important species are sawgrass (*Cladium jamaicense*), beaksedge (*Rhynchospora* spp), Florida little bluestem (*Schizachyrium rhizomatum*), muhly grass (*Muhlenbergia capillaries*), black bogrush (*Schoenus nigricans*) and occasional woody vegetation such as coastal plain willow (*Salix caroliniana*), redbay (*Persea borbonia*), and sweetbay (*Magnolia virginiana*) (Ross,

Mitchell-Bruker, et al. 2006). The study area is very flat, local elevation ranges between 0 and 0.6 meter, and is part of a long term ecological study (Ross et al. 2003; Ross, Mitchell-Bruker, et al. 2006) where permanent transects have been established to document and measure species distribution, soil depth and hydrological parameters across the site.

Classification System and Training Data

Many Florida-wide vegetation classification systems such as the Everglades Vegetation Classification System, Florida Fish and Wildlife Conservation Commission, Florida Gap Analysis Project, Florida Land Use and Cover Classification System and Multi-Species Recovery Project (Rutchey et al. 2006) exist. However, it appears that most of them do not have the preferred level of detail required by the ENP for researching the area's vegetation (Rutchey et al. 2006). Everglades Vegetation Classification System (EVCS) is the most detailed, containing eight major vegetation types: forest, scrub, savanna, prairies and marshes, shrublands, exotics, additional class headings, and special modifiers (Rutchey et al. 2006). The EVCS's "prairies and marshes" vegetation type correspond well to the study area and was used as a foundation for developing classification classes listed in Table 4-1 and Figure 4-2.

Training data were collected in 2009 shortly after the image acquisition date using real time kinematic GPS unit (TOPCON Hiperlite, minimum positional accuracy of 0.1m). A total of 86675 pixels, of which 66430 were used for training and 20245 for accuracy assessment were selected based on 256 field plots measured during May, 2009. The collected point data was randomly distributed in the study area to avoid spatial autocorrelation. Mather (2004) recommended that the number of training data pixels per classification class should be at least 10-30 times the number of feature

classes used in studies with statistical classifiers. Others suggested that DT and ANN classifiers are capable of classifying image data accurately with smaller training set (Hepner et al. 1990; Foody et al. 1995; Pal and Mather 2003). The training and accuracy testing dataset details are presented in Table 4-2.

Imagery

A Microsoft Vexcel UltracamX (UCX) digital fixed array camera was utilized to acquire imagery over the ENP. Microsoft Vexcel UltracamX is a multihead large format sensor and it is capable of providing multispectral imagery by collecting red, green, blue (RGB) and near-infrared (NIR) channels using individual cameras for each band. The imagery was acquired with a solar elevation angle of greater than 30° above the horizon and is cloud and shadow free. The acquisition was done in April 2009, when the wetland communities are in their spring blooming conditions. The imagery was geometrically and radiometrically corrected, pan sharpened (UCX system data level-3), but not orthorectified; however, the geometric distortions due to relief change can be ignored given the minimal elevation relief of the study area (Wolf and Dewitt 2000).

The horizontal positioning accuracy of the imagery is 3.00m at the 95% confidence interval (RMSE = 1.76m given that positional accuracy = 1.7308 * RMSE). Imagery was delivered in the State Plane Coordinate System, Florida East Zone 0901, North American Datum of 1983/High Accuracy Reference Network (HARN) and vertical information is referenced to the North American Vertical Datum of 1988 (NAVD88). Imagery was mosaiced to construct a single image covering the entire study area and clipped to save file space and to eliminate the portion of the images beyond the interested area (Figure 4-1). The main characteristics of the imagery are summarized in Table 4-3.

Texture Features

Spectral features describe the average tonal variations in various bands of the visible and infrared portion of an electromagnetic spectrum, whereas textural features contain information about the spatial distribution of tonal variations within a band (Haralick et al. 1973). First order texture features are derived using first order statistics of local areas. First-order statistics (grey level difference method) estimate the probability density function for differences between neighboring pixels (Carr 1999) using a moving pixel window technique. Using the moving window technique in remote sensing results in a new raster file created from a particular spectral band by using the values of surrounding pixels within a designated area (e.g. a window size of 5 row by 5 column has 25 pixels) to compute a new value of the middle pixel. After each calculation, the window then 'moves' one unit (i.e. column or row) and does the procedure again for every pixel in the area of interest. In this study, every pixel had a data range, mean, variance and entropy so, first order texture value calculated by a window that was moved in the row and column dimensions, one pixel at a time. Second-order statistics describe the frequency with which one gray tone appears in specific relationship to another gray-tone in the image and they are calculated from the grey-level co-occurrence matrix (GLCM) which indicates the probability that each pair of pixel values (*i, j*) co-occur in a given direction and distance (Haralick et al. 1973). These measures are calculated in four directions (horizontal, vertical, left diagonal, right diagonal) on the image and averaged (Haralick et al. 1973).

Classification of Vegetation Communities

Three classification techniques were tested. Maximum likelihood classification algorithm was used as a base method since it is the most widely used and accepted

statistical classification technique (Richards and Jia 2006). Decision tree and ANN classifiers were also employed to develop a high accuracy classification map of the study area.

Decision tree

In this study, the QUEST algorithm was employed to automatically generate decision tree rules. Classification and Regression Trees (CART) algorithm proposed by Breiman et al. (1984) is the most commonly used the remote sensing, however recent studies (Kim and Loh 2001; Sesnie et al. 2008) indicated that QUEST has several advantages over recursive tree construction methods such as CART. Thus, the QUEST algorithm was selected because it is computationally simple and fast, has negligible variable selection bias and produces binary rules (Loh and Shih 1997; Kim and Loh 2001). Kim and Loh (2001) also indicated that when selecting among splitting rules CART is biased in favor of variables that have a large number of possible splits.

The QUEST algorithm selects the split variable based on the computed p-values from an analysis of variance (ANOVA) F-test from the training samples. The variable with the smallest p-value will be selected as the split predictor for the node. Once, the split predictor is established, the splitting point is determined by using the quadratic discriminant analysis (QDA). The QDA algorithm calculates the sample mean and variance for the jth class (j=1, 2) first. Based on the calculated means and variances the QDA splits the X-axis into three intervals $(-\infty, d_1)$, (d_1, d_2) and (d_2, ∞), and selects as split point (d) the one solution between $d_1$and d_2 which is closest to the sample mean for each class (Loh and Shih 1997).

Artificial neural network

Artificial neural networks are models that attempt to process information. They try to replicate the functionality and decision-making processes of the human brain and acquire the knowledge through learning processes and store the gained information in synaptic weights (Haykin 1999). Multi-layer perceptron BP neural network consist of: (1) input layer nodes where external inputs can be fed into the system, (2) one or more hidden layers of computation nodes and (3) one output layer which produces the results of the classification. In the training phase the external input signals consisting of individual band pixel values and texture features were passed through the network via the input layer in a feed-forward manner on a layer-by-layer basis and an output was produced as the actual response of the network. In this *forward pass* process all synaptic weights were assigned randomly and are fixed. In the last phase of the forward pass process, the result is subtracted from the desired results, which was established by the user (i.e. tall sawgrass marsh) once the actual result was generated in the output node. The sum of errors (*E*) is calculated in the following way:

$$E = \frac{1}{2}\sum_{d}\sum_{k}(a_{kd} - o_{kd})^2$$

where a_{kd} is the actual target value, o_{kd} is the predicted class value; associated with the *k*th output unit and training example *d* (Mitchell 1997; Larose 2004). To minimize the error between the actual and the predicted values the output layer sends back the error rate and tries to adjust the weights. Once the error rate was calculated (δ_j), the weights can be updated by:

$$w_{ij,new} = w_{ij,current} + \Delta w_{ij}\ (n)$$

Where w_{ij} represents the weight associated with the *i*th input to node *j* and $\Delta w_{ij}(n) = \eta\delta_j x_{ij} + \alpha\Delta w_{ij}(n-1)$. To calculate the $\Delta w_{ij}(n)$ a positive constant is introduced (η) called the learning rate, ranging between 0 and 1 (usually very close to 0) it helps move the network weights toward an optimal solution (Mitchell 1997) and x_{ij} represents the *i*th input to node *j*. An additional constant, *momentum learning* (α) is added to the weight update rule ($\Delta w_{ij}(n)$), which is used to speed up and stabilize convergence (Mitchell 1997). By employing the equation, the weight update on the *n*th iteration partially depends on the update that occurred during the previous iteration. Normally α should be set between 0 and 1. Smaller values for α would reduce the influence of previous adjustments (Mitchell 1997). In this study the learning rate was set to 0.2 and the momentum learning to 0.3 (Berberoglu et al. 2007).

The following stage, called *backward pass*, consists of the output error being propagated back to the hidden layer. The synaptic weights are then adjusted to make the final output nearer to the expected output (i.e. training classes) (Haykin 1999; Larose 2004). Once the training session is done, the network saves the calculated weights for each input training set. The model uses these weights to classify the new input layers.

Evaluation of Classification Accuracy and Algorithm Comparison

The results of the three employed classification algorithms were evaluated using a confusion matrix. The confusion matrix was calculated based on part of the field measured dataset (Table 4-2), which was split into a training and accuracy assessment dataset. The accuracy dataset (about 1/3 of the collected ground reference data) was used to estimate overall accuracy (percentage of correctly classified pixels), producer's

accuracy, user's accuracy and the Kappa coefficient. The producer's accuracy measures the accuracy of the classified image by computing the number of pixels which were correctly classified into their class. The user's accuracy measures the reliability of the output map in the field, calculating the number of pixels which were incorrectly committed to an incorrect class by the classifier. The overall, producer's and user's accuracies of the developed maps were allocated by five categories: very high accuracy (> 90%), high accuracy (80%-90%), acceptable accuracy (70%- 80%), low accuracy (50%-70%), and poor accuracy (< 50%). The Kappa coefficient estimates the reduction in error generated by the classifier versus the error of a random classifier.

$$\widehat{K} = \frac{p(correct\ classification) - p(chance\ classification)}{1 - p(chance\ classification)}$$

Where p stand for the proportion (Canty 2010). The kappa coefficient ranges between 0 and 1, where 1 indicates a perfect classification. Z-tests were calculated to test that the employed classifier's results differ significantly (Donner et al. 2000). The z-tests were based on the following formula:

$$z = \frac{\widehat{K}_1 - \widehat{K}_2}{(\hat{\sigma}^2_{\widehat{K}_1} + \hat{\sigma}^2_{\widehat{K}_2} - 2\hat{\sigma}_{\widehat{K}_1\widehat{K}_2})}$$

where $\hat{\sigma}_{\widehat{K}_1\widehat{K}_2}$corresponds to the estimated covariance between $\widehat{K}_1$ and $\widehat{K}_2$ (Donner et al. 2000). To determine whether there is a difference between 2 kappa coefficients the null hypothesis of no significance would be rejected at 5% level of significance if |z| >1.96 (Congalton 1991).

Results

Based on the results of Chapter 3, the most promising textural features and window sizes were chosen to validate the classification algorithms accuracy for wetland

graminoid/sedge communities mapping. The tested spectral bands and textural features were the following: spectral bands (red-green-blue-near infrared), NDVI, first order texture features (data range, mean, variance and entropy) calculated by using the 9 by 9 moving window, second order texture features (mean, variance, homogeneity, dissimilarity, entropy and ASM) calculated by using the 7 by 7 GLCM, merged first order texture features (3 by 3 variance and 9 by 9 data range, mean and entropy), merged 3 by 3 and 9 by 9 GLCM second order texture features, and merged first and second order texture features (3 by 3 and 9 by 9). When spectral bands and the NDVI layer were tested with the different classifiers, the results were in a comparable range among all the tested algorithms (Table 4-4).

The artificial neural network classifier (implemented using ITT ENVI v. 4.4) yielded the best overall accuracy of the 3 algorithms when using only the spectral bands for the classification, however, the result produced by the ML classifier was statistically not different ($\alpha \geq 0.05$). The QUEST algorithm (implemented using RuleGen extension v. 1.02 in ITT ENVI v. 4.4) produced a lower overall accuracy with a significantly lower ($\alpha < 0.05$) kappa coefficient (0.63). When the NDVI layer was added to the spectral bands, the overall accuracy values improved in the case of ML and ANN to 75.40% and to 74.53% respectively, however, the DT algorithm's accuracy decreased to 68.89%.

First and second order texture layers were also included in the analysis to further increase the accuracy of the maps. According to Chapter 3, the most promising texture features and window sizes to increase the map accuracy are the data range, mean, variance and entropy in the first order texture measures, while the mean, variance, homogeneity, dissimilarity, entropy and angular second moment performed well in the

second order texture features. The most appropriate window size to discriminate the graminoid and sedge communities are the 9 by 9 pixels moving window in the first order texture and the 7 by 7 pixels GLCM in the second order texture when the texture measures are used without merge. When merging different window sizes, the 3 by 3 pixels and 9 by 9 pixels with the first order texture moving window sizes as well as for the second order texture GLCM are the most suitable (Chapter 3). Moreover, when merging the most appropriate window sizes (3 by 3 pixels and 9 by 9 pixels) in the first order texture features the variance is calculated with the 3 by 3 pixels moving window size while the others (data range, mean and entropy) are calculated with the 9 by 9 pixels moving window size (Chapter 3).

The map accuracy significantly increased compared to the ML classifier result ($\alpha<0.05$) (Tables 4-5 and 4-10), when the QUEST algorithm (DT) and the back-propagation ANN were employed using the 9 by 9 pixels moving window size to develop the vegetation map.

The QUEST algorithm yielded an 84.65% overall map accuracy, with very high detection values for the CM (91.59%), MWP (87.57%) and Woody (100%) classes. The back propagation ANN algorithm further increased the map accuracy to 88.64%, with an excellent detection rate for the CM (97.87%) and Woody (100%) classes and with high detection rate for the MWP (83.44%) and SCWP (81.5%) classes. The comparison of the Kappa coefficients of the QUEST and the BP ANN algorithm also revealed that the BP ANN algorithm delivered a significantly more accurate map ($\alpha<0.05$) (Table 4-10).

When the second order texture features using the 7 by 7 pixels GLCM were tested, the QUEST algorithm yielded a similar overall accuracy value (76.70%) to the

ML classifier (76.89%). The ANN classifier yielded the highest overall accuracy with 81.29%, which is significantly higher than the other classifiers ($\alpha<0.05$) (Table 4-10).

The first tested dataset when the different window sizes were merged was the spectral bands, NDVI and first order texture moving window size (3 by 3 pixels variance and 9 by 9 pixels data range, mean and entropy) data (Table 4-7). There was no statistical difference in the overall accuracy of the map, produced by the ML and DT classifiers, while the ANN classifier produced a significantly higher overall accuracy (89.49%) ($\alpha<0.05$) compared the ML and DT classifier (Table 4-10).

Spectral bands, NDVI and second order texture features (3 by 3 pixels and 9 by 9 pixels GLCM) were also merged and tested (Table 4-8). The QUEST and ANN algorithms yielded a significantly higher overall accuracy (86.89% and 87.95%, respectively) than the ML classifier. The QUEST algorithm delivered very high detection rate for the CM class (95.04%) while the ANN algorithm producer's accuracy was over 80% of all classes.

The four spectral bands, NDVI and first and second order texture features calculated using the 3 by 3 pixels and 9 by 9 pixels moving window and GLCM were merged (n= 45 layers) and tested. The overall accuracy of the DT and ANN classifiers were higher than the ML classifier, however, Kappa coefficient's z-tests revealed that the difference was not significantly different (Tables 4-9 and 4-10).

Discussion

This study was based on the assumption that DT and ANN classifiers can improve classification accuracy for graminoid/sedge wetland communities compared to the ML classifier (Pal and Mather 2003; Berberoglu et al. 2007). Moreover, the inclusion of

textural features beside spectral bands was considered an additional factor in the premise of achieving higher accuracy maps.

Results demonstrated that ANN BP classifier produced significantly more accurate ($\alpha<0.05$) maps in most of the examined cases where ML or QUEST algorithms were used. However, when only spectral bands and NDVI layer were included in the analysis, the ANN and ML algorithms produced maps with comparable accuracy (74.53% vs. 75.40%) while the QUEST algorithm underperformed compared to the ANN and ML classifiers. In fact, the QUEST DT algorithm produced less accurate maps in all but one trial in this study. The best result was produced by the QUEST algorithm using the spectral bands, NDVI layer and the merged 3 by 3 and 9 by 9 window second order texture features. However, even with this high overall accuracy, the resulting maps were not statistically more accurate than those of produced by the ML or the ANN BP classifiers. The QUEST algorithm significantly improved the accuracy of the vegetation map only once versus the ML classifier, when the spectral bands, NDVI, and the first order texture features (9 by 9 window) were included. Similarly to Sesnie et al. (2008) the QUEST algorithm produced low overall accuracy when only the spectral bands were included in the mapping (71%) and further decreased when only the NDVI layer was added (69%), but results increased when textural information was incorporated. Sesnie et al. (2008) achieved 93% overall accuracy when using 12 spectral and geospatial layers, however, they used low spatial resolution imagery (Landsat TM), and also noted that overall accuracy result increased when less heterogeneous land cover was mapped. In this study, the highest overall accuracy for the QUEST algorithm was 86.89%, which is lower than Sesnie et al. (2008) achieved. However, their wetland

categories were less detailed consisting only of palm swamps, forested swamps and herbaceous swamps.

Artificial neural network classifier consistently produced high accuracy results for the study area. Yet, when only the spectral bands and NDVI layer were included in the classification, the output was not significantly better than the ML classifier. However, as texture features were added in the classification, the produced vegetation maps accuracies increased significantly in all trials but one, compared to the ML and DT classifiers. Also, the highest overall accuracy (89.49%) was achieved when using the ANN with spectral bands, NDVI layer and merged first order texture features (3 by 3 pixel window variance and 9 by 9 pixel window data range, mean, entropy). The second highest overall accuracy was produced with the combination of spectral bands, NDVI layer and a first order texture features 9 by 9 moving window (88.64%). This set of data contained the same number of layers (9), however, the pre-processing of the data was simpler and faster, as only one moving window size was calculated and merged with the spectral bands and NDVI layer. The consistently high accuracy results can be attributed with the ANN algorithm's generalization capability, which is the ability of the algorithm to obtain accurate outputs for new input data that is different from the training data (Zhang et al. 2003). Berberoglu et al. (2004) also noted that the generalization capability of the ANN is a key advantage against the ML classifier, especially in areas where the spectral difference among vegetation cover attributes is small.

When examining the individual plant communities' accuracies, results reveal that the ANN algorithm detected the classes with the highest accuracy. For example, ANN has no less than 80% producer's accuracy and over 74.94% user's accuracy for all

classes when used to classify the spectral bands, NDVI layer and first order texture features (3 by 3 window variance and 9 by 9 window data range, mean and entropy). The Woody vegetation class was always detected easily and accurately, which is understandable based on the very different spectral signature from the other classes. However, the importance of the texture's window size beside the classification algorithm is evident when individual class accuracies are reviewed. The ANN classifier generated 70.31% producer's accuracy for the CWP class when the 9 by 9 window size first order texture was included in the analysis, but the produce's accuracy for the same class increased to 82.06% when the 3 by 3 window size first order texture variance was included beside the 9 by 9 window size. This can be due to the heterogeneity of CWP class, where several plant species compose the community.

The MWP and SCWP classes also showed similar trends, in the ML and DT classification but they were more consistent with the ANN classifier. When the second order texture features (7 by 7 window) were tested together with the spectral bands and NDVI layer, the CWP class' producer's accuracies were low (<66.77%) in all tested classification algorithms, which implies that the 7 by 7 window second order texture measures did not characterized the communities accurately enough. However, similarly to the first order texture windows, when the 3 by 3 and 9 by 9 GLCM window second order texture measures were merged with the spectral bands and NDVI layer, the classification results increased with all the employed classification algorithms, but still they were lower compared to the merged first order texture features (3 by 3 and 9 by 9 window), spectral bands and NDVI layer. Moreover, when the second order texture features were merged with the spectral bands, NDVI layer and first order texture

measures, the producer's and user's accuracy decreased, similarly to the overall accuracy, for the communities that used the DT and the ANN classifier compared to the merged layers of spectral bands, NDVI layer and first order texture measures.

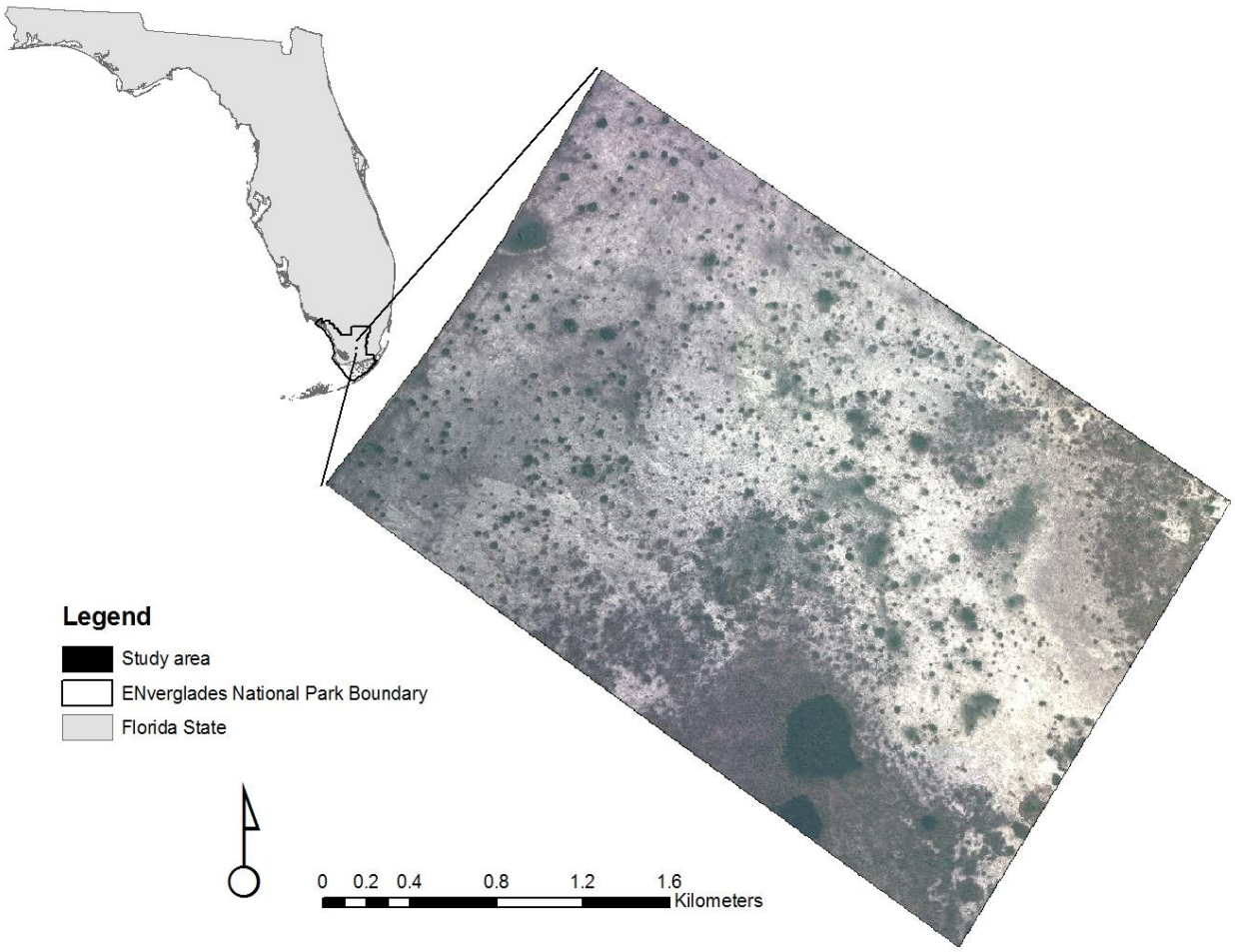

Figure 4-1. UltacamX mosaiced image of the study area in the Everglades National Park. The scale bar refers to the image.


A.


B.

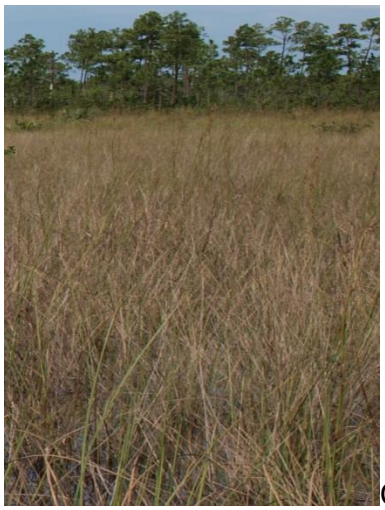
C.


D.


E.

Figure 4-2. Example images of the classification classes. A. - Tall sawgrass marsh, B. - Short sawgrass wet prairie, C. - Schizachyrium wet prairie, D. - Muhlenbergia wet prairie, E. - Woody vegetation.

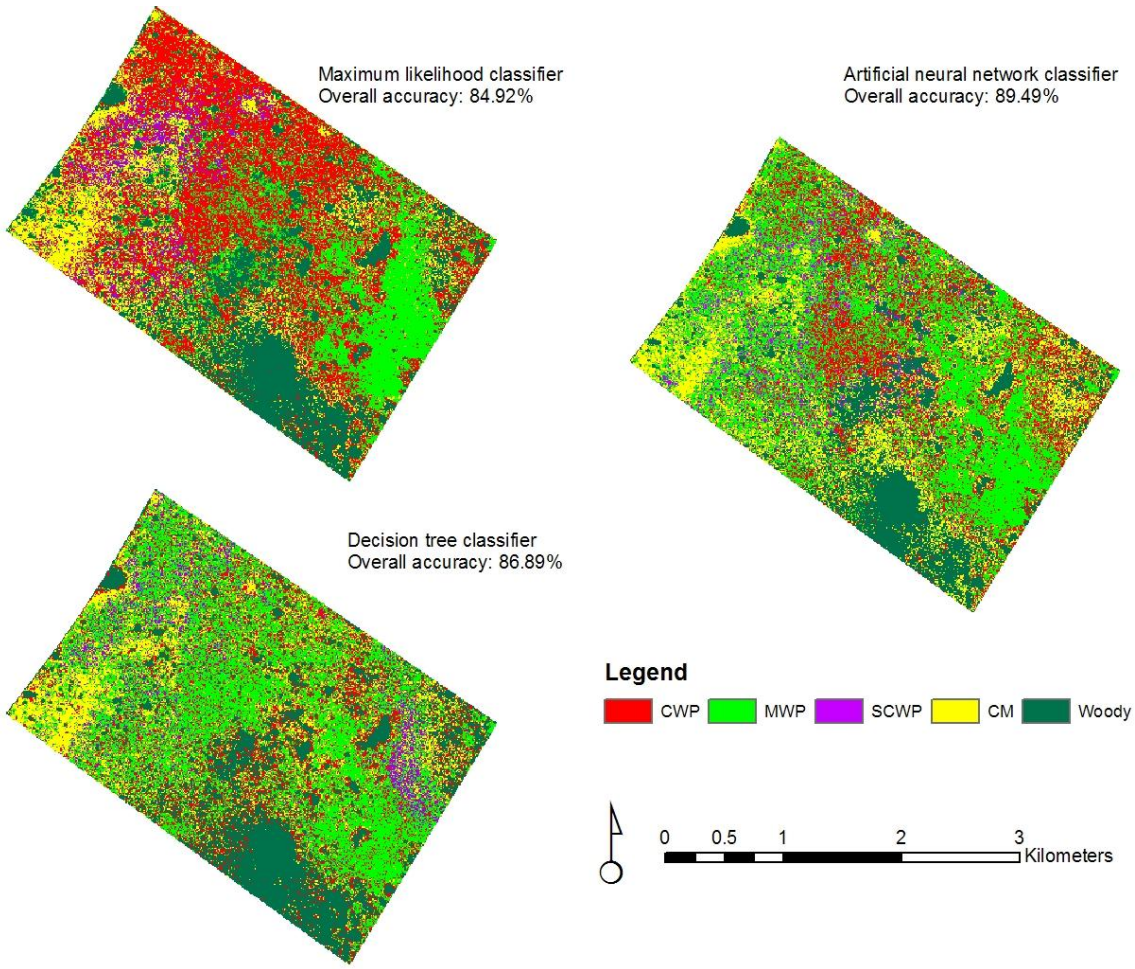

Figure 4-3. Plant community maps of the study area in the Everglades National Park using different classification algorithms. Spectral bands, NDVI layer and second order texture features (3 by 3 and 9 by 9 window sizes) for the maximum likelihood and decision tree classifiers, while spectral bands, NDVI layer and first order texture features (3 by 3 window variance and 9 by 9 window data range, mean, entropy) for the artificial neural network classifier were used. CM - Tall sawgrass marsh, CWP - Short sawgrass wet prairie, MWP - Muhlenbergia wet prairie, SCWP - Schizachyrium wet prairie, Woody - Woody vegetation.

Table 4-1. Major plant communities in the research area.

Class name	Dominant plant species
Tall sawgrass marsh (CM)	*Cladium jamaicense,* some *Eleocharis cellulosa* and *Typha domengensis* Pers.
Short sawgrass wet prairie (CWP)	*Cladium jamaicense, some Rhynchospora* spp., *Schoenus nigricans, Schizachyrium rhizomatum*
Schizachyrium wet prairie (SCWP)	*Schizachyrium rhizomatum*, *Cladium jamaicense*
Muhlenbergia wet prairie (MWP)	*Muhlenbergia capillaries, Schizachyrium rhizomatum, Schoenus nigricans, Cladium jamaicense*
Woody vegetation (Woody)	*Salix caroliniana, Persea borbonia, Magnolia virginiana*

Table 4-2. Description of collected ground reference data.

Classes	Number of points collected	Number of pixels were selected for training	Number of pixels selected for accuracy testing	Average number of pixels in a training/accuracy polygon
CM	48	12536	3237	328
CWP	60	14733	4730	324
SCWP	36	12782	3856	462
MWP	56	12940	3737	297
Woody	56	13439	4685	323

CM - Tall sawgrass marsh, CWP - Short sawgrass wet prairie, MWP - Muhlenbergia wet prairie, SCWP - Schizachyrium wet prairie, Woody - Woody vegetation.

Table 4-3. UltracamX imagery data characteristics.

Sensor	Microsoft Vexcel UltracamX
Acquisition date	March 28 – April 10, 2009
Flight altitude	4115 ± 90 meter
Spectral resolution	Red (580 …. 700 nanometer) Green (480 …. 630 nanometer) Blue (410 …. 570 nanometer) Near Infrared (690 …. 1000 nanometer)
Spatial resolution	0.305 meter
Data	Spectral Bands Derived Texture Features
Radiometric resolution	14 bit
Area covered by one image	4400 m x 2870
Overlap	60% forward lap 40% side lap

Table 4-4. Classification results based on spectral bands and the NDVI layer.

	Spectral bands	Spectral bands and NDVI layer
Maximum likelihood		
Overall accuracy (%)	73.8070	75.4016
Decision Tree		
Overall accuracy (%)	71.1348	68.8957
Artificial Neural Network		
Overall accuracy (%)	74.4250	74.5316

Table 4-5. Spectral bands, NDVI and first order texture features (9 pixels by 9 pixels moving window) classification results.

Class	ML		DT		ANN	
	PA	UA	PA	UA	PA	UA
CM	70.33	79.92	91.59	91.78	97.87	89.49
CWP	81.85	57.03	62.06	67.32	70.31	73.48
MWP	75.74	62.63	87.57	66.15	83.44	77.22
SCWP	39.75	81.96	69.81	97.79	81.50	95.25
Woody	99.92	100.00	100.00	97.13	100.00	99.17
Overall accuracy (%)	74.0884		84.6514		88.6412	

PA - producer's accuracy(%), UA - user's accuracy(%), ML - maximum likelihood classifier, DT - decision tree classifier, ANN - multi-layer perceptron back-propagation artificial neural network classifier, CM - Tall sawgrass marsh, CWP - Short sawgrass wet prairie, MWP - Muhlenbergia wet prairie, SCWP - Schizachyrium wet prairie, Woody - Woody vegetation.

Table 4-6. Spectral bands and NDVI and second order texture features (7 pixels by 7 pixels GLCM) classification results.

Class	ML		DT		ANN	
	PA	UA	PA	UA	PA	UA
CM	85.65	71.26	57.37	80.93	69.32	80.43
CWP	66.77	76.20	62.60	54.66	60.09	81.21
MWP	59.71	61.97	89.86	59.46	89.26	61.92
SCWP	70.24	76.05	68.86	95.73	75.09	89.75
Woody	100.00	93.93	94.58	94.31	99.24	97.80
Overall accuracy (%)	76.8963		76.7023		81.2926	

PA - producer's accuracy(%), UA - user's accuracy(%), ML - maximum likelihood classifier, DT - decision tree classifier, ANN - multi-layer perceptron back-propagation artificial neural network classifier, CM - Tall sawgrass marsh, CWP - Short sawgrass wet prairie, MWP - Muhlenbergia wet prairie, SCWP - Schizachyrium wet prairie, Woody - Woody vegetation.

Table 4-7. Spectral bands and NDVI and first order texture features (3 pixels by 3 pixels variance and 9 pixels by 9 pixels data range, mean, entropy moving window) classification results.

Class	ML		DT		ANN	
	PA	UA	PA	UA	PA	UA
CM	90.31	79.23	92.20	91.37	97.37	95.39
CWP	70.22	84.39	59.28	66.90	82.06	74.94
MWP	72.77	78.79	86.97	63.93	82.84	75.93
SCWP	85.08	76.45	66.56	96.66	80.51	94.99
Woody	100.00	100.00	100.00	97.13	99.88	99.56
Overall accuracy (%)	84.0192		83.6031		89.4962	

PA - producer's accuracy(%), UA - user's accuracy(%), ML - maximum likelihood classifier, DT - decision tree classifier, ANN - multi-layer perceptron back-propagation artificial neural network classifier, CM - Tall sawgrass marsh, CWP - Short sawgrass wet prairie, MWP - Muhlenbergia wet prairie, SCWP - Schizachyrium wet prairie, Woody - Woody vegetation.

Table 4-8. Spectral bands, NDVI and second order texture features merged 3 pixels by 3 pixels and 9 pixels by 9 pixels GLCM window classification results.

Class	ML		DT		ANN	
	PA	UA	PA	UA	PA	UA
CM	94.36	86.60	95.04	92.46	87.04	91.58
CWP	75.35	81.75	75.07	66.85	86.55	79.75
MWP	65.89	77.93	87.02	74.12	83.69	71.62
SCWP	87.96	76.54	70.62	97.81	80.14	94.82
Woody	99.97	100.00	100.00	97.13	99.64	99.36
Overall accuracy (%)	84.9279		86.8906		87.9593	

PA - producer's accuracy(%), UA - user's accuracy(%), ML - maximum likelihood classifier, DT - decision tree classifier, ANN - multi-layer perceptron back-propagation artificial neural network classifier, CM - Tall sawgrass marsh, CWP - Short sawgrass wet prairie, MWP - Muhlenbergia wet prairie, SCWP - Schizachyrium wet prairie, Woody - Woody vegetation.

Table 4-9. Spectral bands, NDVI and first and second order texture features 3 pixels by 3 pixels and 9 pixels by 9 pixels moving window and GLCM classification results.

Class	ML		DT		ANN	
	PA	UA	PA	UA	PA	UA
CM	95.85	84.41	94.73	90.00	87.95	87.24
CWP	71.83	81.98	56.68	61.42	76.59	76.18
MWP	69.21	75.75	89.31	70.79	82.99	70.90
SCWP	83.78	77.24	70.17	97.31	77.35	96.40
Woody	100.00	100.00	100.00	97.13	100.00	97.17
Overall accuracy (%)	83.9782		85.1094		86.3308	

PA - producer's accuracy(%), UA - user's accuracy(%), ML - maximum likelihood classifier, DT - decision tree classifier, ANN - multi-layer perceptron back-propagation artificial neural network classifier, CM - Tall sawgrass marsh, CWP - Short sawgrass wet prairie, MWP - Muhlenbergia wet prairie, SCWP - Schizachyrium wet prairie, Woody - Woody vegetation.

Table 4-10. Kappa confidences and significance testing based on the z-score for maps using various combinations of input layers and classifiers.

	Comparison of Kappa Coefficients (Standard error)					
	Classifier		Classifier		Classifier	
Model	ML	DT	ML	ANN	DT	ANN
SB	0.6716** (0.0042)	0.6303 (0.0072)	0.6716	0.6740 (0.0069)	0.6303	0.6740**
SB+NDVI	0.6915** (0.0041)	0.6013 (0.0073)	0.6915	0.6755 (0.0069)	0.6013	0.6755**
SB+NDVI+FO 9x9	0.6758 (0.0042)	0.8055** (0.0046)	0.6758	0.8560** (0.0041)	0.8055	0.8560**
SB+NDVI+SO 7x7	0.7107 (0.0036)	0.7056 (0.0054)	0.7107	0.7622** (0.0050)	0.7056	0.7622**
SB+NDVI+FO 3x3 variance, 9x9 data range, mean, entropy	0.8000 (0.0035)	0.7921 (0.0047)	0.8000	0.8671** (0.0039)	0.8055	0.8671**
SB+NDVI+SO 3x3 and 9x9	0.8114 (0.0034)	0.8343 (0.0043)	0.8114	0.8476** (0.0042)	0.8343	0.8476
SB+NDVI+FO 3x3 and 9x9+SO 3x3 and 9x9	0.7993 (0.0035)	0.8113 (0.0046)	0.7993	0.8268 (0.0044)	0.8113	0.8268

SB - spectral bands, NDVI - normalized difference vegetation index, FO - first order texture features, SO - second order texture features, 3x3 - 3 by 3 pixels window size, 9x9 - 9 by 9 pixels window size, ML - maximum likelihood classifier, DT - decision tree classifier, ANN - neural network classifier. ** - significantly different based on the z-test. Differences are significant at the 95% confidence level (|z| >1.96) (Congalton 1991). No asterisk means not statistically different.

CHAPTER 5
CONCLUSIONS

This study has shown that the spatial heterogeneity of different vegetation cover in a wetland environment can be mapped accurately using high resolution aerial imagery. Beside spectral bands, inclusion of an NDVI layer, derived texture features and classification algorithms improved the accuracy of the derived map.

The results of this study support the use of first order texture features in high accuracy mapping of very complex, heterogeneous wetlands plant communities. Results also show that first order texture features have a higher impact on the increased mapping accuracy when using ANN than the second order texture features. Second order texture features had similar producer's and user's accuracies for the plant communities as the first order texture features, but the overall accuracy tended to be lower. Also, it is simpler to calculate first order texture features than employing the GLCM for calculating second order texture features. When first and second order texture features and NDVI were included, beside spectral bands, into the classification; overall accuracy increased.

Also, the moving window size is a very important consideration, where the appropriate size plays a crucial role in the developed map's accuracy. The applied window size must depend on the communities of interest. When the semivariogram method was used to estimate the most appropriate window size, its results generally indicated the proper window size. However, trials with other window sizes revealed that the window size estimated using the semivariogram did not necessary generate the highest accuracy map. Thus, a careful selection is very important when choosing the right window sizes for texture derivation.

In this study two plant community classes reacted very differently to window's size changes. The Tall sawgrass class (CM) had very low accuracy values when a small window size has been used to calculate first order texture features while the Schizachyrium wet prairie (SCWP) class had high producer's accuracy. When the moving window size was gradually increased, the accuracy of detecting CM class increased and decreased in the case of the SCWP class. Thus, when more complex classes are involved in the classification, smaller window size might be more appropriate.

The classification algorithms produced different results. The highest classification accuracy was achieved with the ANN classifier (89.49%), which is very close the 90% accuracy standard that is expected by the RECOVER monitoring and assessment plan (RECOVER 2004). The DT classifier, when texture measures were included produced similar or higher overall accuracies than the ML classifier. However its computing time was significantly higher. When only spectral bands were tested, the ML classifier had similar results as the ANN or DT classifiers, but overall, maps based on the spectral bands and NDVI layer only had low overall accuracies.

Future research should focus on the inclusion of ancillary data such as soil depth, high resolution digital elevation models and hydrological variables to further improve classification accuracies. Additionally, the developed methodology allows for not only the monitoring of the investigated plant communities, but other communities of interest could be included as well, such as the native but spreading cattail (*Typha* spp.) or monitoring of invasive plant species such as melaleuca (*Melaleuca quinquenervia*) or Brazilian pepper (*Schinus terebinthifolious*).

High spatial resolution imagery is an important factor when classifying plant communities. This is especially important since some of the plant communities in this study occupied small localized patches, which cannot be delineated with lower resolution imagery. The developed methodology is repeatable, thus it can be used with a new set of imagery for change detection studies. The thematic vegetation map can also serve to better analyze spatial patterns of the studied vegetation communities, identify habitats of interest and help determine wetland areas that are susceptible to change.

LIST OF REFERENCES

Armentano TV, Sah JP, Ross MS, Jones DT, Cooley HC, Smith CS (2006) Rapid responses of vegetation to hydrological changes in Taylor Slough, Everglades National Park, Florida, USA. Hydrobiologia 569: 293–309

Ashish D, McClendon RW, Hoogenboom G (2009) Land-use classification of multispectral aerial images using artificial neural networks. International Journal of Remote Sensing 30: 1989–2004

Baker C, Lawrence R, Montagne C, Patten D (2006) Mapping wetlands and riparian areas using Landsat ETM+ imagery and decision-tree-based models. Wetlands 26: 465–474

Balaguer A, Ruiz LA, Hermosilla T, Recio JA (2010) Definition of a comprehensive set of texture semivariogram features and their evaluation for object-oriented image classification. Computers & Geosciences 36: 231–240

Baraldi A, Parmiggiani F (1995) An Investigation of the Textural Characteristics Associated with Gray Level Cooccurrence Matrix Statistical Parameters. IEEE Transactions on Geoscience and Remote Sensing 33: 293–305

Barbosa I (2010) Mapping Wetland Environments in the Brazilian Savannah From High Resolution IKONOS Image Data. In: Wagner W, Székely B (eds) ISPRS TC VII Symposium. pp. 62–67

Belluco E, Camuffo M, Ferrari S, Modenese L, Silvestri S, Marani A, Marani M (2006) Mapping salt-marsh vegetation by multispectral and hyperspectral remote sensing. Remote sensing of environment 105: 54–67

Benediktsson JA, Swain PH, Ersoy OK (1993) Conjugate-gradient neural networks in classification of multisource and very-high-dimensional remote sensing data. International Journal of Remote Sensing 14: 2883–2903

Berberoglu S, Yilmaz KT, Ozkan C (2004) Mapping and monitoring of coastal wetlands of Cukurova Delta in the Eastern Mediterranean region. Biodiversity and Conservation 13: 615–633

Berberoglu S, Curran PJ, Lloyd CD, Atkinson PM (2007) Texture classification of Mediterranean land cover. International Journal of Applied Earth Observation and Geoinformation 9: 322–334

Bernhardt CE, Willard DA (2009) Response of the Everglades ridge and slough landscape to climate variability and 20th-century water management. Ecological Applications 19: 1723–1738

Breiman L, Friedman J, Stone C, Olshen R (1984) Classification and regression trees. Chapman & Hall, New York, NY, USA

Brinson MM, Malvárez AI (2002) Temperate freshwater wetlands: types, status, and threats. Environmental Conservation 29: 115–133

Bullock A, Acreman M (2003) The role of wetlands in the hydrological cycle. Hydrology and Earth System Sciences 7: 358–389

Bwangoy JRB, Hansen MC, Roy DP, Grandi GD, Justice CO (2010) Wetland mapping in the Congo Basin using optical and radar remotely sensed data and derived topographical indices. Remote Sensing of Environment 114: 73–86

Canty MJ (2010) Image Analysis, Classification, and Change Detection in Remote Sensing: With Algorithms for ENVI/IDL, Second Edition. CRC Press, Boca Raton, FL, USA

Carr J (1999) Classification of digital image texture using variograms. In: Atkinson PM, Tate NJ (eds) Advances in remote sensing and GIS analysis. Wiley, West Sussex, UK, pp. 135–146

Carr JR, de Miranda FP (1998) The Semivariogram in Comparison to the Co-Occurrence Matrix forClassification of Image Texture. IEEE Transactions on Geoscience and Remote Sensing 36: 1945–1953

Childers DLD, Jones RF, Noe R, Rugge GB, Scinto M, Leonard J (2003) Decadal change in vegetation and soil phosphorus pattern across the Everglades landscape. Journal of Environmental Quality 32: 344–362

Clausi DA (2002) An analysis of co-occurrence texture statistics as a function of grey level quantization. Canadian Journal of remote sensing 28: 45–62

Coburn CA, Roberts ACB (2004) A multiscale texture analysis procedure for improved forest stand classification. International Journal of Remote Sensing 25: 4287–4308

Congalton RG (1991) A review of assessing the accuracy of classifications of remotely sensed data. Remote sensing of environment 37: 35–46

Craft C, Vymazal J, Richardson C (1995) Response of everglades plant communities to nitrogen and phosphorus additions. Wetlands 15: 258–271

Curran PJ (1988) The semivariogram in remote sensing: an introduction. Remote Sensing of Environment 24: 493–507

Dahl TE (2006) Status and trends of wetlands in the conterminous United States 1998 to 2004. U.S. Department of the Interior; Fish and Wildlife Service, Washington, D.C., USA

Davis SM (1994) Phosphorus inputs and vegetation sensitivity in the Everglades. In: Davis SM, Ogden JC (eds) Everglades: The Ecosystem and Its Restoration. St. Lucie Press, Delray Beach, FL, USA, pp. 357–378

Davis SM, Ogden JC (eds) (1994) Everglades: The Ecosystem and Its Restoration. St. Lucie Press, Delray Beach, FL, USA

Davis SM, Gaiser EE, Loftus WF, Huffman AE (2005) Southern marl prairies conceptual ecological model. Wetlands 25: 821–831

Davis SM, Gunderson LH, Park WA, Richardson JR, Mattson JE (1994) Landscape dimension, composition, and function in a changing Everglades ecosystem. In: Davis SM, Ogden JC (eds) Everglades: The Ecosystem and Its Restoration., pp. 419–444

Dell'Acqua F, Gamba P, Trianni G (2006) Semi-automatic choice of scale-dependent features for satellite SAR image classification. Pattern recognition letters 27: 244–251

Dillabaugh K, King D (2008) Riparian marshland composition and biomass mapping using Ikonos imagery. Canadian Journal of Remote Sensing 34: 143–158

Donner A, Shoukri MM, Klar N, Bartfay E (2000) Testing the equality of two dependent kappa statistics. Statistics in Medicine 19: 373–387

Doren RF, Armentano TV, Whiteaker LD, Jones RD (1997) Marsh vegetation patterns and soil phosphorus gradients in the Everglades ecosystem. Aquatic Botany 56: 145–163

Doren RF, Rutchey K, Welch R (1999) The Everglades: a perspective on the requirements and applications for vegetation map and database products. Photogrammetric Engineering and Remote Sensing 65: 155–161

Duever M (2006) South Florida Vegetation Classification Scheme. Crosswalks. http://ufdc.ufl.edu/UF00066304/00001. Accessed 13 Jun 2011

Duever MJ (2005) Big Cypress regional ecosystem conceptual ecological model. Wetlands 25: 843–853

Erwin KL (2008) Wetlands and global climate change: the role of wetland restoration in a changing world. Wetlands Ecology and Management 17: 71–84

Foody GM (2004) Thematic map comparison: evaluating the statistical significance of differences in classification accuracy. Photogrammetric Engineering and Remote Sensing 70: 627–634

Foody GM, McCulloch MB, Yates WB (1995) The effect of training set size and composition on artificial neural network classification. International Journal of Remote Sensing 16: 1707–1723

Franklin SE, Wulder MA, Lavigne MB (1996) Automated derivation of geographic window sizes for use in remote sensing digital image texture analysis. Computers & Geosciences 22: 665–673

Friedl MA, Brodley CE (1997) Decision tree classification of land cover from remotely sensed data. Remote Sensing of Environment 61: 399–409

Fuller DO (2005) Remote detection of invasive Melaleuca trees (Melaleuca quinquenervia) in South Florida with multispectral IKONOS imagery. International Journal of Remote Sensing 26: 1057–1063

Ge S, Carruthers R, Gong P, Herrera A (2006) Texture Analysis for Mapping Tamarix parviflora Using Aerial Photographs along the Cache Creek, California. Environmental Monitoring and Assessment 114: 65–83

Ghedira H, Bernier M, Ouarda TBMJ (2000) Application of neural networks for wetland classification in RADARSAT SAR imagery. In: Geoscience and Remote Sensing Symposium, 2000. Proceedings. IGARSS 2000. IEEE 2000 International, pp. 675–677

Gilmore MS, Wilson EH, Barrett N, Civco DL, Prisloe S, Hurd JD, Chadwick C (2008) Integrating multi-temporal spectral and structural information to map wetland vegetation in a lower Connecticut River tidal marsh. Remote Sensing of Environment 112: 4048–4060

Gluck M, Rempel R, Uhlig P (1996) An evaluation of remote sensing for regional wetland mapping applications. Forest Research Report, Ontario Forest Research Institute, Sault Ste Marie, Ontario, Canada

Goel PK, Prasher SO, Patel RM, Landry JA, Bonnell RB, Viau AA (2003) Classification of hyperspectral data by decision trees and artificial neural networks to identify weed stress and nitrogen status of corn. Computers and Electronics in Agriculture 39: 67–93

Goodin DG, Henebry GM (1997) A technique for monitoring ecological disturbance in tallgrass prairie using seasonal NDVI trajectories and a discriminant function mixture model. Remote Sensing of Environment 61: 270–278

Gunderson LH (1997) Vegetation of the Everglades: determinants of community composition. In: Davis SM, Ogden JC (eds) Everglades: The Ecosystem and Its Restoration. CRC Press, Baca Raton, FL, pp. 323–340

Gunderson LH, Loftus WF (1993) The Everglades. In: Martin WH, Boyce SG, Echternacht AC (eds) Biodiversity of the Southeastern United States. John Wiley and Sons, New York, NY, USA. pp. 199–255

Hancock PJ, Boulton AJ, Humphreys WF (2005) Aquifers and hyporheic zones: towards an ecological understanding of groundwater. Hydrogeology Journal 13: 98–111

Haralick RM, Dinstein I, Shanmugam K (1973) Textural features for image classification. IEEE Transactions on systems, man, and cybernetics 3: 610–621

Harvey JW, McCormick PV (2009) Groundwater's significance to changing hydrology, water chemistry, and biological communities of a floodplain ecosystem, Everglades, South Florida, USA. Hydrogeology Journal 17: 185–201

Harvey KR, Hill GJE (2001) Vegetation mapping of a tropical freshwater swamp in the Northern Territory, Australia: A comparison of aerial photography, Landsat TM and SPOT satellite imagery. International Journal of Remote Sensing 22: 2911–2925

Haykin S (1999) Neural networks: a comprehensive foundation. Prentice Hall, Upper Saddle River, NJ, USA

Hepner G, Logan T, Ritter N, Bryant N (1990) Artificial Neural Network Classification Using a Minimal Training Set: Comparison to Conventional Supervised Classification. Photogrammetric Engineering and Remote Sensing 56: 469–473

Johansen K, Coops NC, Gergel SE, Stange Y (2007) Application of high spatial resolution satellite imagery for riparian and forest ecosystem classification. Remote sensing of Environment 110: 29–44

Joria P (2001) A Review of Present Applications of Remote Sensing Technology for the Mapping of Large River Floodplains and Wetland Cover Types. U.S. Geological Survey, Upper Midwest Environmental Sciences Center, La Crosse, WI, USA

Journal Citation Reports Thomson Reuters Web of Knowledge. http://wokinfo.com/. Accessed 23 Apr 2011

Junk WJ, Brown M, Campbell IC, Finlayson M, Gopal B, Ramberg L, Warner BG (2006) The comparative biodiversity of seven globally important wetlands: a synthesis. Aquatic Sciences 68: 400–414

Kass GV (1980) An Exploratory Technique for Investigating Large Quantities of Categorical Data. Applied Statistics 29: 119–127

Kim H, Loh WY (2001) Classification trees with unbiased multiway splits. Journal of the American Statistical Association 96: 589–604

Kindscher K, Fraser A, Jakubauskas ME, Debinski DM (1997) Identifying wetland meadows in Grand Teton National Park using remote sensing and average wetland values. Wetlands Ecology and Management 5: 265–273

Knight JF, Lunetta RS (2003) An experimental assessment of minimum mapping unit size. IEEE Transactions on Geoscience and Remote Sensing 41: 2132–2134

Kushlan JA (1990) Freshwater marshes. In: Myers RL, Ewel JJ (eds) Ecosystems of Florida. University of Central Florida Press, Orlando, FL, pp. 324–363

Larose DT (2004) Discovering Knowledge in Data: An Introduction to Data Mining. John Wiley & Sons Ltd, Chichester, UK

Larsen L, Aumen N, Bernhardt C, Engel V, Givnish T, Hagerthey S, Harvey J, Leonard L, McCormick P, Mcvoy C, Noe G, Nungesser M, Rutchey K, Sklar F, Troxler T, Volin J, Willard D (2011) Recent and Historic Drivers of Landscape Change in the Everglades Ridge, Slough, and Tree Island Mosaic. Critical Reviews in Environmental Science and Technology 41: 344–381

Lloyd CD, Berberoglu S, Curran PJ, Atkinson PM (2004) A comparison of texture measures for the per-field classification of Mediterranean land cover. International Journal of Remote Sensing 25: 3943–3965

Lockwood JL, Ross MS, Sah JP (2003) Smoke on the water: the interplay of fire and water flow on Everglades restoration. Frontiers in Ecology and the Environment 1: 462–468

Loh WY, Shih YS (1997) Split selection methods for classification trees. Statistica sinica 7: 815–840

Lu D, Weng Q (2007) A survey of image classification methods and techniques for improving classification performance. International Journal of Remote Sensing 28: 823–870

Madden M, Jones D, Vilchek L (1999) Photointerpretation Key for theEverglades Vegetation Classification System. Photogrammetric Engineering & Remote Sensing 65: 171–177

Maheu-Giroux M, Blois S (2005) Mapping the invasive species Phragmites australis in linear wetland corridors. Aquatic Botany 83: 310–320

Marella RL (2009) Water Withdrawals, Use, and Trends in Florida, 2005. Scientific Investigations Report, Florida Department of Environmental Protection, U.S. Department of the Interior, U.S. Geological Survey, Reston, VA, USA

Mas JF (2004) Mapping land use/cover in a tropical coastal area using satellite sensor data, GIS and artificial neural networks. Estuarine, Coastal and Shelf Science 59: 219–230

Mas JF, Flores JJ (2008) The application of artificial neural networks to the analysis of remotely sensed data. International Journal of Remote Sensing 29: 617–663

Mather P (2004) Computer processing of remotely sensed images: an introduction. John Wiley & Sons, Chichester West Sussex, England

Maxa M, Bolstad P (2009) Mapping northern wetlands with high resolution satellite images and LiDAR. Wetlands 29: 248–260

Michishita R, Xu B, Gong p (2008) A decision tree classifier for the monitoring of wetland vegetation using Aster data in the Poyang lake region, China. In: The International Archives of the Photogrammetry, Remote Sensing and Spatial Information Sciences. Beijing, China, p. 8

Mitchell TM (1997) Machine Learning. McGraw-Hill Inc. New York, NY, USA

Mitsch W, Gosselink J (2007) Wetlands. Wiley, Hoboken, NJ, USA

Moody A, Gopal S, Strahler AH (1996) Artificial neural network response to mixed pixels in coarse-resolution satellite data. Remote Sensing of Environment 58: 329–343

Nicholls RJ, Hoozemans FMJ, Marchand M (1999) Increasing flood risk and wetland losses due to global sea-level rise: regional and global analyses. Global Environmental Change 9: S69–S87

Nielsen EM, Prince SD, Koeln GT (2008) Wetland change mapping for the US mid-Atlantic region using an outlier detection technique. Remote Sensing of Environment 112: 4061–4074

Ogden JC (2005) Everglades ridge and slough conceptual ecological model. Wetlands 25: 810–820

Ogden L (2004) Ecosystems or Landscapes, Public Participation in Environmental Decision Making: A Case Study in the Florida Everglades. In: Knowledge of Landscapes to Landscaping Action. Cemegref, Bordeaux, France, p. 10

Olmsted IC, Armentano TV (1997) Vegetation of Shark Slough, Everglades National Park. Technical Report, South Florida Natural Resources Center, Everglades National Park

Olmsted IC, Loope LL, Rinze RE (1980) A survey and baseline analysis of aspects of the vegetation of Taylor Slough, Everglades National Park. Everglades National Park South Florida Research Center, Homestead, FL, USA

Ouma Y, Tetuko J, Tateishi R (2008) Analysis of co-occurrence and discrete wavelet transform textures for differentiation of forest and non-forest vegetation in very-high-resolution optical-sensor imagery. International Journal of Remote Sensing 29: 3417–3456

Ozesmi SL, Bauer ME (2002) Satellite remote sensing of wetlands. Wetlands Ecology and Management 10: 381–402

Pal M, Mather PM (2003) An assessment of the effectiveness of decision tree methods for land cover classification. Remote sensing of environment 86: 554–565

Paola JD, Schowengerdt RA (1995) A Detailed Comparison of Backpropagation Neural Network and Maximum-Likelihood Classifiers for Urban Land Use Classification. IEEE Transactions on Geoscience and Remote Sensing 33: 981–997

Paul S, Küsel K, Alewell C (2006) Reduction processes in forest wetlands: tracking down heterogeneity of source/sink functions with a combination of methods. Soil Biology and Biochemistry 38: 1028–1039

Pearlstine L, Portier KM, Smith SE (2005) Textural discrimination of an invasive plant, Schinus terebinthifolius, from low altitude aerial digital imagery. Photogrammetric Engineering & Remote Sensing 71: 289–298

Pearlstine LG, Pearlstine EV, Aumen NG (2010) A review of the ecological consequences and management implications of climate change for the Everglades. Journal of the North American Benthological Society 29: 1510–1526

Puig J, Hyman G, Bolanos S (2002) Digital Classification vs. Visual Interpretation: a case study in humid tropical forests of the Peruvian Amazon. In: XXIX International Symposium on Remote Sensing of Environment. Buenos Aires, Argentina, p. 5

Puissant A, Hirsch J, Weber C (2005) The utility of texture analysis to improve per-pixel classification for high to very high spatial resolution imagery. International Journal of Remote Sensing 26: 733–745

Quinlan J (1993) C4.5: programs for machine learning. Morgan Kaufmann Publishers, San Mateo, CA, USA

RECOVER (2004) CERP monitoring and assessment plan: Part1 monitoring and supporting research. United States Army Corps of Engineers, Jacksonville, FL, USA and South Florida Water Management District, West Palm Beach, FL, USA

Reed P (1988) National list of plant species that occur in wetlands: national summary. Biological Report, National Ecology Research Center, St. Petersburg, FL, USA

Richardson CJ, Huvane JK (2008) Ecological status of the Everglades: environmental and human factors that control the peatland complex on the landscape. Everglades Experiments: 13–58

Richardson C (2010) The Everglades: North America's subtropical wetland. Wetlands Ecology and Management 18: 517–542

Richards J, Jia X (2006) Remote sensing digital image analysis an introduction. Springer, Berlin, Germany

Ross MS, Sah JP, Ruiz PL, Jones DT, Cooley H, Travieso R, Tobias F, Snyder JR, Hagyari D (2006) Effect of hydrologic restoration on the habitat of the Cape Sable seaside sparrow

Ross MS, Reed DL, Sah JP, Ruiz PL, Lewin MT (2003) Vegetation: environment relationships and water management in Shark Slough, Everglades National Park. Wetlands Ecology and Management 11: 291–303

Ross MS, Mitchell-Bruker S, Sah JP, Stothoff S, Ruiz PL, Reed DL, Jayachandran K, Coultas CL (2006) Interaction of hydrology and nutrient limitation in the Ridge and Slough landscape of the southern Everglades. Hydrobiologia 569: 37–59

Rutchey K, Schall T, Sklar F (2008) Development of vegetation maps for assessing Everglades restoration progress. Wetlands 28: 806–816

Rutchey K, Schall T, Doren R, Atkinson A, Ross M, Jones D, Madden M, Vilchek L, Bradley K, Snyder J, Burch J, Pernas T, Witcher B, Pyne M, White R, Smith T, Patterson M, Gann G (2006) Vegetation Classification for South Florida Natural Areas. Open-File Report, United States Geological Survey, Saint Petersburg, FL

Rutchey K, Godin J (2009) Determining an appropriate minimum mapping unit in vegetation mapping for ecosystem restoration: a case study from the Everglades, USA. Landscape Ecology 24: 1351–1362

Sader SA, Ahl D, Liou WS (1995) Accuracy of landsat-TM and GIS rule-based methods for forest wetland classification in Maine. Remote Sensing of Environment 53: 133–144

Schmidt KS, Skidmore AK (2003) Spectral discrimination of vegetation types in a coastal wetland. Remote Sensing of Environment 85: 92–108

Sesnie SE, Gessler PE, Finegan B, Thessler S (2008) Integrating Landsat TM and SRTM-DEM derived variables with decision trees for habitat classification and change detection in complex neotropical environments. Remote Sensing of Environment 112: 2145–2159

Sklar FH, van der Valk A (2002) What we know and should know about tree islands. In: van der Valk A, Sklar FH (eds) Tree Islands of the Everglades. Kluwer Academic Publishers, Dordrecht, The Netherlands, pp. 499–522

Smith GM, Spencer T, Murray AL, French JR (1998) Assessing seasonal vegetation change in coastal wetlands with airborne remote sensing: an outline methodology. Mangroves and Salt Marshes 2: 15–28

St-Louis V, Pidgeon AM, Radeloff VC, Hawbaker TJ, Clayton MK (2006) High-resolution image texture as a predictor of bird species richness. Remote sensing of environment 105: 299–312

Stober QJ, Scheidt D, Jones R, Thornton K, Ambrose R, France D (1996) South Florida Ecosystem Assessment Interim Report. United States Environmental Protection Agency

Stokstad E (2008) Florida: Big Land Purchase Triggers Review of Plans to Restore Everglades. Science 321: 22

Swain PH, Hauska H (1977) The decision tree classifier: design and potential. IEEE Transactions on Geoscience Eectronics GE-15: 142–147

Titus JG, Richman C (2001) Maps of lands vulnerable to sea level rise: modeled elevations along the US Atlantic and Gulf coasts. Climate Research 18: 205–228

Tso B, Mather PM (2009) Classification methods for remotely sensed data. CRC Press, Boca Raton, FL, USA

USFWS (1999) Freshwater marshes and wet prairies. South Florida multi-species recovery plan - Ecological communities. http://www.fws.gov/verobeach/images/pdflibrary/marshes%20wet%20prairies.pdf , Accessed 23 Apr 2011

Walker R, Solecki W (2004) Theorizing Land-Cover and Land-Use Change: The Case of the Florida Everglades and Its Degradation. Annals of the Association of American Geographers 94: 311–328

Wang L, Sousa WP, Gong P, Biging GS (2004) Comparison of IKONOS and QuickBird images for mapping mangrove species on the Caribbean coast of Panama. Remote Sensing of Environment 91: 432–440

Waser LT, Baltsavias E, Ecker K, Eisenbeiss H, Feldmeyer-Christe E, Ginzler C, Küchler M, Zhang L (2008) Assessing changes of forest area and shrub encroachment in a mire ecosystem using digital surface models and CIR aerial images. Remote Sensing of Environment 112: 1956–1968

Welch R, Remillard M, Doren RF (1995) GIS Database Development for South Florida'sNational Parks and Preserves. Photogrammetric Engineering & Remote Sensing 61: 1371–1381

Willard DA, Bernhardt CE, Holmes CW, Landacre B, Marot M (2006) Response of Everglades tree islands to environmental change. Ecological Monographs 76: 565–583

Winter TC (1999) Relation of streams, lakes, and wetlands to groundwater flow systems. Hydrogeology Journal 7: 28–45

Wolf P, Dewitt B (2000) Elements of photogrammetry: with applications in GIS. McGraw-Hill, Boston, MA, USA

Wright C, Gallant A (2007) Improved wetland remote sensing in Yellowstone National Park using classification trees to combine TM imagery and ancillary environmental data. Remote Sensing of Environment 107: 582–605

Wulder MA, LeDrew EF, Franklin SE, Lavigne MB (1998) Aerial Image Texture Information in the Estimation of Northern Deciduous and Mixed Wood Forest Leaf Area Index (LAI). Remote Sensing of Environment 64: 64–76

Yang CC, Prasher SO, Enright P, Madramootoo C, Burgess M, Goel PK, Callum I (2003) Application of decision tree technology for image classification using remote sensing data. Agricultural Systems 76: 1101–1117

Yang X (2007) Integrated use of remote sensing and geographic information systems in riparian vegetation delineation and mapping. International Journal of Remote Sensing 28: 353–370

Zedler JB (2000) Progress in wetland restoration ecology. Nature 15: 402–407

Zedler JB (2003) Wetlands at your service: reducing impacts of agriculture at the watershed scale. Frontiers in Ecology and the Environment 1: 65–72

Zhang S, Liu HX, Gao DT, Wang W (2003) Surveying the methods of improving ANN generalization capability. In: Machine Learning and Cybernetics, 2003 International Conference, pp. 1259–1263

Zweig CL, Kitchens WM (2008) Effects of landscape gradients on wetland vegetation communities: information for large-scale restoration. Wetlands 28: 1086–1096

BIOGRAPHICAL SKETCH

Zoltan Szantoi, son of Zoltan Szantoi and Erzsebet Pap, was born in 1977 in Szentes, Hungary. He and his brother, Robert Szantoi were reared on a small tomato and cauliflower farm in Csanytelek, Hungary. In June 1995, he graduated from Janos Bartha Horticultural High School. He attended Istvan Barsony Environmental Technician School in Csongrad, Hungary and graduated in 1997. He then entered Samuel Tessedik College, Szarvas, Hungary in September, 1997 and graduated with a Bachelor of Science degree in environmental agricultural engineering in June 2001. During 2001 to 2002, he worked as an intern at the Heritage Seedling Inc. in Salem, Oregon. Working in the industry for one year after the internship, he entered the School of Forestry and Wildlife, Auburn University, in January 2004 and earned a Master of Science degree in 2006. In 2007, he was accepted as a PhD. graduate student at the University of Florida and graduated in 2011.